A nanofluidic device for visualizing dynamic biopolymer interactions *in vitro*

Gilead Henkin

Department of Physics

McGill University, Montreal

December 14, 2016

A thesis presented to McGill University in partial fulfillment of the requirements of the degree of Masters of Science

ACKNOWLEDGMENTS

The work herein presented is the result of close collaboration and teamwork. I thank Chris McFaul for introducing me to the lab technology and getting me started on CLiC experiments. Dan Berard is responsible for building much of the equipment used, and the fabrication methods I have used and detailed were only performed in frequent consultation with him. Frank Stabile has been a close teammate on many experimental fronts, putting particular effort into the DNA transfer experiments. Shane Scott and Jill Laurin assisted with abundant biological knowledge, and were generous with their skills in biomolecular protocols. Marjan Shayegan provided useful research experience and in particular developed the expertise needed in nano-confined enzymatic experiments. Jason Leith provided invaluable advice in experiment and theory including assistance with the text of the first manuscript. Albert Kamanzi and I collaborated closely when learning fabrication techniques. Adriel Arsenault worked closely with all of us, having expertise with optics, especially the dual-view system. Caleb Guthrie, Alvin Liao, and Yash Patel provided essential support on software. Francois Michaud wrote the code that I adapted to analyze my experiments, and provided support during analysis.

An additional thanks to the rest of the Leslie Lab throughout my time at McGill for making the lab a bright place to work, especially during the dark winter.

Elsewhere, I'd like to thank Amani Hariri for sharing her expertise on single molecule fluorescence measurements, Janane Rahbani for consultation on DNA samples, and Professor Hanadi Sleiman for supervising my exchange work in her laboratory. The scientists at ZS Genetics - William Glover, Larry Scipioni, Felipe Guzman - provided expertise and invaluable advice to the projects. The McGill nanotools facility made all this work possible and accessible, and the staff - Sasa Ristic, John Li, and Lino Eugene in particular - were generous with their time and expertise in fabrication. Boris Le Drogoff provided help with fabricating nanochannels at INRS Varennes.

I would like to thank the sources of funding for this work: NSERC, CREATE Train-

ing Program in Bionanomachines (CTPB) for my fellowship, CMC Microsystems for a fabrication grant, ZSGenetics, Micralyne.

Prefacing the text of each manuscript is a list of specific contributions of the authors to the work. Thanks to Shane Scott and Pam Austin who helped with translating.

And especially: thank you to Sabrina Leslie, who guided all the research I completed during my Master's degree.

ABSTRACT

As biological physics develops at the level of single-molecule studies, new tools are required to make observations at micrometer and nanometer scales. Many methods have been developed in the past decade offering unprecedented control and resolution at these lengthscales - for example, novel fluorescent techniques such as fluorescence resonance energy transfer (FRET) probe nanoscale interactions, and optical tweezers or atomic force microscopy (AFM) measure forces with exquisite sensitivity. However, the ability to simultaneously control and measure molecules at this scale remains a great challenge, often requiring physical restraint of molecules on a surface or other limiting modifications. Towards realizing new experimental regimes allowing control and measurement of less-constrained molecules, we present a novel micro- and nanofluidic device for controlling and visualizing DNA interactions. A previously-developed method for confining DNA into nanochannels, Convex Lens-induced Confinement (CLiC), is modified with fabricated structures allowing dynamic exchange of small reagents during confinement. Use of this device is demonstrated through a series of vignette experiments. First, we present a series of experiments examining the interaction between DNA complexed with the fluorescent dye YOYO-1 and buffer solutions with varying ionic strength. We find evidence for different fluorescent binding modes by simultaneously measuring polymer length and fluorescent intensity as the molecules react to the ionic strength change in real time. We follow with short preliminary studies observing dynamic compaction by a cationic surfactant and cleavage by several restriction enzymes. We then present an application of this device in which we use a binding agent to selectively deposit stretched DNA onto a silica surface, potentially useful for examining DNA samples under higher-resolution microscopes such as AFM or SEM.

ABRÉGÉ

À mesure que la physique biologique se développe au niveau des études de molécules uniques, de nouveaux outils sont nécessaires pour effectuer des observations au micrométre et des échelles nanométriques. De nombreuses méthodes ont été développées au cours de la dernière dcennie et offrent un contrôle et une résolution sans précédent à ces échelles de longueur. Par exemple, de nouvelles techniques fluorescentes telles que les interactions nanoscopiques de la sonde de transfert de l'énergie de résonance de fluorescence (FRET) et les microscopies à force atomique (AFM) avec une sensibilité exquise. Cependant, la capacité de contrôler et de mesurer simultanément des molécules à cette échelle reste un grand défi, nécessitant souvent une immobilisation physique des molécules sur une surface ou d'autres modifications limitantes. En vue de réaliser de nouveaux régimes expérimentaux permettant le contrôle et la mesure de molécules moins contraintes, nous présentons un nouveau dispositif micro et nanofluidique pour contrler et visualiser les interactions ADN. Une méthode développée précédemment pour confiner l'ADN dans des nanochannels, Confinement Convexe Lentille-induit (CLiC), est modifiée avec des structures fabriquées permettant un échange dynamique de petits réactifs pendant la contrainte. L'utilisation de ce dispositif est démontrée par une série d'expériences de vignette. Premièrement, nous présentons une série d'expériences examinant l'interaction entre l'ADN complexé avec le colorant fluorescent YOYO-1 et des solutions médiateurs avec une force ionique variable. Nous trouvons des preuves de différents modes de liaison fluorescente en mesurant simultanément la longueur du polymère et l'intensité fluorescente lorsque les molécules réagissent au changement de force ionique en temps réel. Nous suivons avec de courtes études préliminaires observant le compactage dynamique par un tensioactif cationique et le clivage par plusieurs enzymes de restriction. On présente ensuite une application de cette appareil dans lequel on utilise un agent liant pour déposer sélectivement de l'ADN étiré sur une surface de

silice, potentiellement utile pour examiner des échantillons d'ADN sous des microscopes à résolution plus élevée tels que AFM ou SEM.

Contents

List of Figures

List of Acronyms

AFM - Atomic force microscopy

APTES - Aminopropyl triethoxysilane

BME - β-mercaptoethanol

CLiC - Convex lens-induced confinement

CTAB - Cetyl trimethylammonium bromide

CTMA - Cetyl trimethylammonium

DNA - Deoxyribonucleic acid

DTT - Dithiothreitol

EMCCD - Electron multiplying charge coupled device

FOCS - 1H,1H,2H,2H-perfluorooctyldimethylchlorosilane

FRET - Fluorescent resonant energy transfer, or Förster resonant energy transfer

NA - Numerical aperture

PCA - Protocatechuic acid

PCD - Protocatechuate-3,4-dioxygenase

PDMS - Polydimethyl siloxane

PEG - Polyethylene glycol

PVP - Polyvinylpyrrolidone

SEM - Scanning electron microscopy

TBE - Tris/Borate/EDTA buffer

TEM - Transmission electon microscope

TIRF - Total internal reflection fluorescence

UV - Ultra violet

Chapter 1

Single molecule DNA experiments in micro- and nanofluidics: a brief literature review

1.1 Introduction

The diversity of the current state of biophysics owes a lot to decades of groundbreaking research in the biological sciences. Since the structure of DNA was solved more than 60 years ago, biology has seen multiple revolutions in knowledge and technique. DNA as a biomolecule, as a code, and as a polymer continues to prove worthy of deep study. The past decade in particular has seen large developments of measurements at the single molecule level, which has the ability to measure rare events or subpopulations that would get lost in a bulk average. Fluorescent techniques have enabled exquisite resolution of DNA reactions under optical microscopes, using micro- and nano-scale fabrication techniques developed for semiconductor technologies to create customized nanostructured environments to control the molecules[1].

DNA deserves the spotlight it holds in the natural sciences. It is an exercise in cryptography [2], coding not only an entire organism, but a highly specific organism, in a linear sequence of 4 letters. It is a demonstration of polymer theory [3, 4], a material easily derived from any species and holding, on average, consistent characteristics. It is a biomolecule with a huge – and unknown – number of specific and complex interactions to support life [5, 6, 7]. Precise manipulation of DNA at the single molecule scale is a very attractive way to measure many of these properties and effects. Putting it under a microscope to just 'look at the thing', as Feynman said, answers questions much more quickly than making inferences from bulk spectrometry or other less sensitive measures. This desire has coupled well with advancements in the semi-conductor industry - the same methods used to manufacture circuitry for computers are well-compatible with microscopy glass. This has led to microfluidics fabricated to the micro- and nanoscale for fluorescence microscopy purposes, as described further in this review and in the following chapters [8, 9, 10, 11].

One common limitations to these methods is the inability to simultaneously control a reaction at nanometer scales and visualize it. This is due to the great difficulty of introducing reagents to a small fluidic space. This thesis provides an avenue towards overcoming this outstanding difficulty, by modifying existing techniques to allow dynamic manipulation of molecules at the nanoscale.

1.2 DNA-protein interactions

Within the cell, DNA is part of complex machinery along with other biomolecules, including proteins. There has accumulated over the years a good deal of knowledge of different proteins and their specificity, inhibitors, and activators [5]. However, it has become of special interest to reveal the nanoscale mechanics of these DNA-protein interactions. We may know one protein inhibits another, but we might not be able to reveal any mechanis-

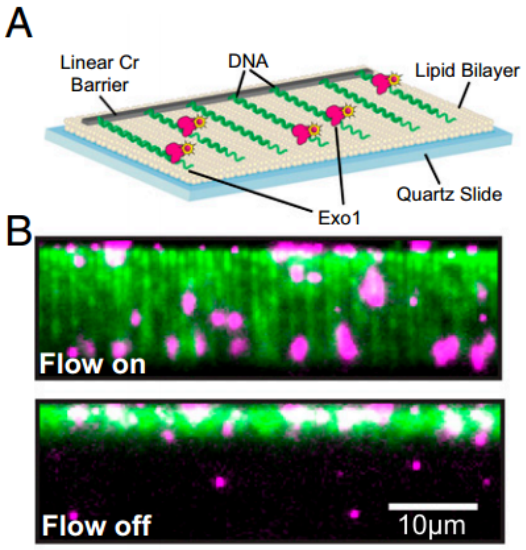

Figure 1.1: DNA-protein interaction visualization with DNA curtains. (A) Schematic of the experimental setup. DNA is bound to a strip of chromium and sits on a lipid bilayer. Fluid flow extends the DNA molecules. (B) Fluorescence images show DNA with and without fluid flow (green) with bound protein (pink). Reproduced from Myler *et al*[12]

tic detail or information about the trajectory of the interaction from a bulk assay. Myler *et al* recently published a study using single molecule methods to extract such detail [12]. The study used a method called DNA curtains, in which DNA are bound to a strip of chromium and rest on a lipid bilayer, extending under liquid flow as shown in figure 1.1. The flow can be used to introduce any molecules desired (e.g. chemical reagents or proteins), making it well-suited for high-throughput DNA-protein interaction studies.

Myler *et al* use this method to explore the activity of Exo1, an enzyme that digests or resections DNA. Figure 1.2 demonstrates use of this method to examine the activity of Exo1 on a DNA strand. Fluorescence microscopy provides non-ambiguous indication of not only single proteins bound to DNA, but their translocation velocity, and dissociation. Further results indicate that RPA, another DNA-binding protein, influences the activity of Exo1 by displacing the Exo1 by binding at the same location. The DNA curtains experiment provides valuable information on the mechanism of inhibition or activation, as bulk

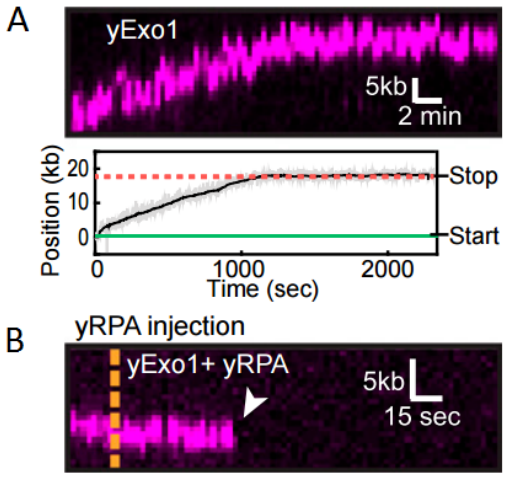

Figure 1.2: Kymogram of the position of Exo1 protein (pink) bound to DNA with (B) and without (A) the presence of RPA protein.Reproduced from Gorman *et al*[13]

assays were unclear. In some instances, RPA inhibits by blocking Exo1, while in others, RPA activates Exo1 by forcing its dissociation and reassociation at different points. This is a prime example of how single molecule measurements reveal the entire trajectory of a protein-DNA interaction.

In a separate study using the same technique of DNA curtains, Gorman *et al* similarly track the trajectory of a DNA-associated protein, MutSα, which is known to target and repair mis-matched sites in the sequence of double-stranded DNA [13]. Single molecule fluorescence microscopy techniques allowed them to rigorously show how after binding to DNA, MutSα diffuses in 1D until it finds the mismatch site, and at that point recruits another protein which alters its conformation so it does not stop at that site again. DNA curtains clearly shows great potential for tracking proteins diffusing along the length of DNA and introducing chemicals to react with the complex. However, it does have its limitations: the lipid bilayer system is cumbersome to prepare for experiments, and because the DNA is imaged under flow, it is not free to explore much of its conformational space. It is known that biomolecular functions are intimately related to structure - indeed,

this is one of the driving motivators of biophysical sciences.

An interesting experiment by Forget and Kowalczykowski uses optical tweezers to apply some control to DNA conformation to explore some of that space in respect to DNA repair protein RecA [14]. RecA mediates DNA repair by the well-studied process of homologous recombination. Though well studied, the mechanism of RecA's search for homologous template sites is not known.

Preparation of RecA-DNA filaments of various lengths gave the ability to test a hypothesis that the extended filament performs a 3D search. They were able to find that the chance of a filament finding the homologous sites decreases by stretching the molecule out, and also by decreasing the length of the filament, indicating that conformation is important for activity: the homologous section must be well within the volume that a filament is able to sample1.3.

Single molecule fluorescence microscopy has also been used to investigate protein interaction with DNA in live cells. Gebhardt *et al* expressed various proteins with fluorescent labels in cells to investigate how they move in the cell[15]. Because the cell is so densely packed with proteins, they used an ultra-thin sheet of light to illuminate a 2D section of the sample, using a method called reflected light sheet microscopy (RLSM). Measuring diffusion of proteins, they inferred when proteins were bound to DNA versus diffusing through the cell, and were also able to resolve colocalization of proteins.

Common bench procedures can be done in a single-molecule device, such as restriction mapping. Riehn *et al* [16] showed this possibility in 100nm nanochannels etched in glass. DNA was incubated with proteins previous to loading in the device - importantly, proteins were selected that would bind to their restriction sites without needing the magnesium that also drives the cutting. DNA is electrophoretically driven into nanochannels, into which magnesium can easily diffuse and enable restriction to occur. The benefit of doing this in a nanoconfining single molecule device is being able to map cuts in a DNA from averaging only a handful of copies, and it is immediately known where each restric-

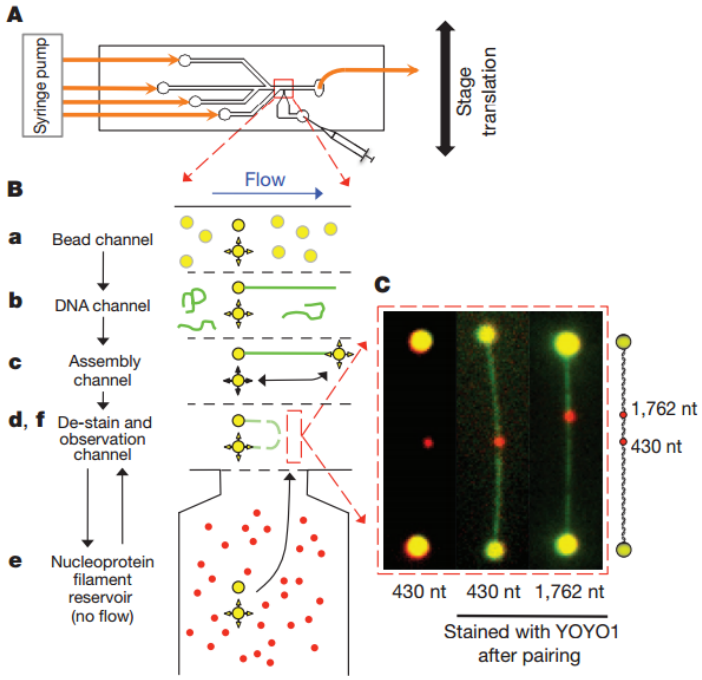

Figure 1.3: (A) Schematic of the microfluidic chip, etched with a carbon dioxide laser in glass. (B) Schematic of experimental procedure. Streptavidin-coated beads are trapped with optical tweezers and brought into a channel filled with biotinylated λphage DNA. With one DNA bound, a second bead is attached to the other end of the DNA, providing the ability to control end-to-end distance of the polymer. The DNA is then destained and introduced to a chamber of RecA filaments, now ready for imaging. (C) Fluorescent images of beads (yellow), DNA (green), and RecA filaments (red) of various lengths. The nucleotide (nt) lengths correspond to specific homologous pairs of sites on the lambda sequence, where the fluorescing RecA filament is bound. Reproduced from Forget *et al*[14].

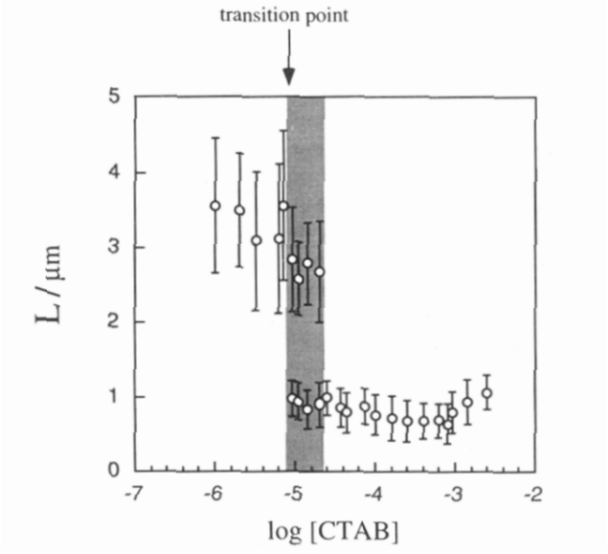

Figure 1.4: DNA undergoing a coil to globule transition with increasing concentration of CTAB, a cationic surfactant. L measures the largest cross section of T4-phage DNA molecules in solution, as they are not constrained to nanochannels. Reproduced form Mel'nikov *et al* [17].

tion fragment belongs in the sequence.

1.3 DNA interactions with other molecules

Single molecule fluorescence measurements were also used to examine interactions of other molecules with DNA, which tend to be not specific to sequence. Mel'nikov *et al* [17] introduced a striking transition of DNA when complexed with a cationic surfactant: the positive charges associate with the negatively charged DNA backbone and the non-polar cetyl tails cause it to precipitate and collapse on itself. The DNA thereby condenses from an extended random coil into a smaller globule. Their experiments were done on DNA in uncontrolled configurations, where the reactions are generally performed in bulk conditions, and then adhered to a surface. This severely restricts the ability to capture true dynamics.

Single molecule measurements allowed detection of a coexistence region between the

random coil and globule conformations. This differs from the process of other compaction events as measured by Yoshikawa *et al* [18]. In this paper, they mixed DNA with a poly-ethylene glycol (PEG), a neutral polymer, that has been complexed with a positively charged amino group. This chemical also induced transition, by a different method. When the positive charge associates with the DNA, the long PEG chain competes with DNA for volume, and with enough concentration forces the DNA to compact. However, they show that during the course of this compaction, a long DNA chain compacts partly before compacting all the way - it is no longer an all-or-none interaction, and a coexistence does not describe the dynamics. Interestingly, PEG without this amino group [19] does exhibit the all-or-none transition, with a similar coexistence region. Perhaps the electrostatic association with the amino group actually hinders the progress of the reaction by limiting the configurations that the polymers can take, a non-obvious result. These different dynamic processes would look similar in bulk spectroscopy, highlighting once more the benefit of single molecule fluorescent measurement.

It is also of interest how DNA reacts to buffer conditions, which have strong effects on biological reactions. Reisner *et al* [20] performed experiments measuring the extension of DNA in nanochannels after incubating in buffers of varying ionic strength. They found a strong dependence of extension on ionic strength, measured with different channel widths to determine new parameters in the confinement theory. However, as these were performed by incubating the molecules prior to loading into nanochannels and measuring, any dynamic information of a reaction has been lost. Especially as the salt is also expected to have an effect on the electrostatically associated dye used to visualize the DNA, further exploration of this would help clarify the true relationship that salt has with DNA.

1.4 Conclusions

This is a small window into the ways that single molecule fluorescent measurement has been used to explore important biological reactions. Often results expose physical properties of an experiment that are otherwise inaccessible. In particular, these methods hold great promise for efficient mapping of 'macroscopic' structure of genomes [21, 22, 23], such as kilobasepair-scale rearrangements and deletions, by identifying and matching specific points along a sequence. These methods offer a way to map large-scale structure in one measurement, rather than averaging over thousands of smaller measurements. With the additional advantage of advances in microfabrication processes, this field has a lot of innovation left in it, as measurements are made at smaller and smaller lengthscales with higher and higher precision. At the same time, existing technologies are limited by often confining DNA to surfaces or to manipulated beads, and are often unable to control the reaction process during visualization of the effect due to the difficult of fluidics control at these scales.

1.5 A single-molecule DNA reactor

The literature referenced in the preceding sections demonstrates the breadth of work in the field of single-molecule techniques in studying DNA. However, the outstanding challenge of controlling DNA conformation during introduction of reagents, for high resolution in time and space, remains. In the next chapter, we present a manuscript detailing our experimental work to overcome this challenge, modifying previous techniques, and present three demonstration experiments[24]. Contributions of individual authors are detailed in the appendix.

All experiments are performed using an inverted fluorescence microscope, allowing imaging of multiple laser lines. The optical set-up is detailed in figure 1.5. The experiments detailed are performed leveraging the previously published technique of Convex Lens-induced Confinement (CLiC)[25, 26], mounted above the inverted microscope objective on a movable stage. This device is shown in figure 1.6. Briefly, a microns-thin flow cell held in place by an acrylic microfluidic chuck is compressed at a single point by a convex lens, which is positioned by an additional XY stage. A piezo actuator on the convex lens Z-axis allows precise positioning of the lens on the nanometer scale, thereby enabling precise control over the height of the fluidic chamber. In particular, when the height is sufficiently low, confined molecules are limited to configurations determined by the glass surfaces, allowing dramatic linearization and extension in nanochannels. This entropically-driven effect allows gentle confinement of long DNA molecules, while the thin glass of the flow cell allows high-resolution fluorescence imaging.

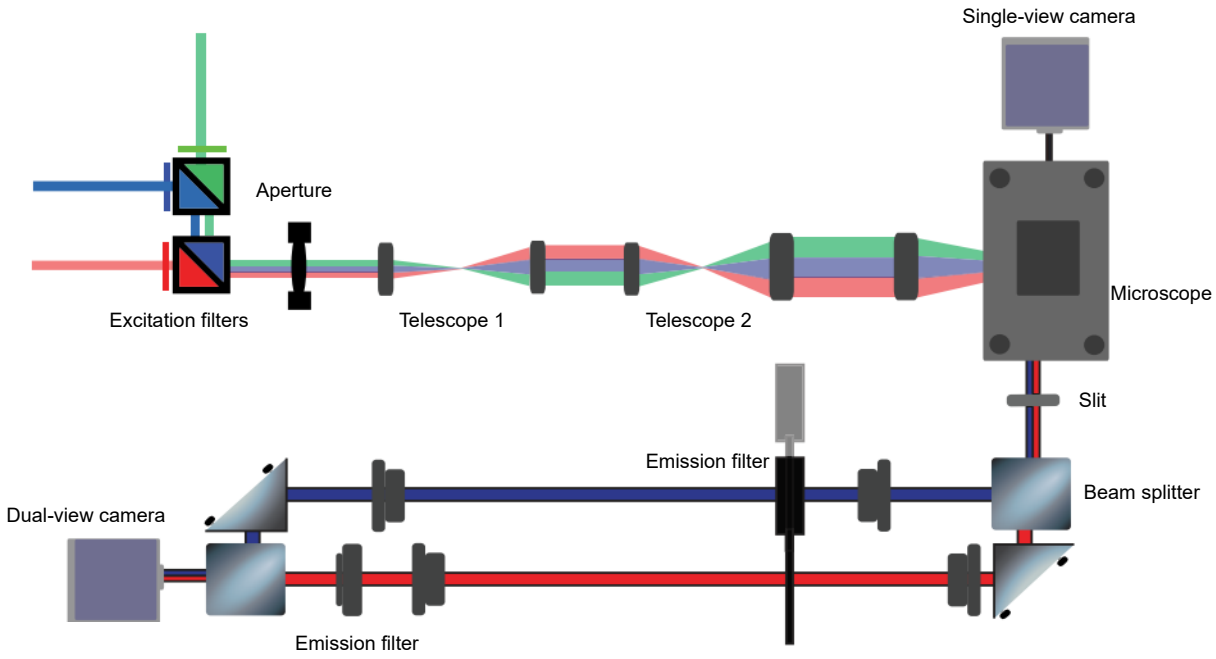

Figure 1.5: Simplified schematic of microscope optics, adapted from Arsenault *et al* [27]. Not to scale. All experiments herein are performed with this optical system, allowing for three laser lines for different excitation wavelengths, and with a dual-view system for spectrally separating simultaneously fluorescing molecules. The telescopes in the excitation pathway enlarge the beam to maximize the width of the illuminated field. The slit narrows the emission image such that corresponding but spectrally-separate images may hit the EMCCD camera at the same time.

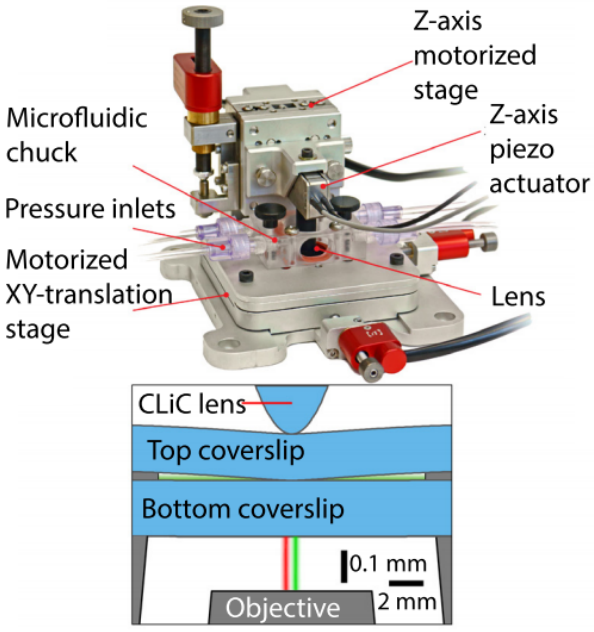

Figure 1.6: Adapted from Berard *et al*[28]. CLiC device used in all experiments, with schematic of confinement. The microfluidic chuck holds a flow cell in place on an XY-translation stage above an inverted microscope objective, and allows interfacing with inlet holes in the flow cell. A convex lens mounted on a piezo actuator is brought into contact with the top coverslip, compressing the fluidic chamber.

Chapter 2

Manipulating and visualizing molecular interactions in customized nanoscale spaces

Gil Henkin, Daniel Berard, Francis Stabile, Marjan Shayegan, Jason S. Leith, Sabrina R. Leslie

2.1 Abstract

We present a dynamically adjustable nanofluidic platform for formatting the conformations of and visualizing the interactions between biomolecules in solution. To illustrate, we visualize and manipulate salt-induced, surfactant-induced, and enzyme-induced reactions between small-molecule reagents and DNA molecules, where the conformations of the DNA molecules are formatted by the imposed nanoscale confinement. In response to dynamically modifying the local salt concentration, we report two salt-induced transitions in DNA molecules which occur on separate timescales: a rapid change in polymer extension due to modified local ionic screening; and a gradual change in polymer

brightness, reflecting release of intercalated YOYO-1 dye. Our time-resolved measurements provide new insights into the influence of YOYO-1 dye on polymer stiffness. In response to introducing cationic surfactants in solution, we temporally resolve single-molecule compaction trajectories of DNA polymers, guided by the confining nanogroove environment; this is in contrast to the uncontrolled collapse which would occur in free solution under similar conditions. In the presence of restriction enzymes, we directly visualize the cleavage of multiple DNA sites under adjustable nanoscale confinement. By using nanofabricated, non-absorbing, low-background glass walls to confine biopolymers, our nanofluidic platform facilitates quantitative exploration of physiologically and biotechnologically relevant processes at the nanoscale.

2.2 Introduction

As fluorescence microscopy has advanced to the point of single-molecule resolution, there is growing interest in visualizing and quantitatively understanding biochemical mechanisms at the nanoscale. Single-molecule microscopy of DNA molecules undergoing dynamic processes and interactions inside nanoscale volumes, such as DNA condensation in the presence of proteins or crowding agents, can provide important mechanistic insights into physiological processes occurring under confinement, such as in the dense nucleus of a cell. Further, recent studies show that *in vitro* nanoconfinement of enzymatic processes can enhance reactivity[29]. Single-DNA manipulation and visualization techniques represent the cutting edge of not only discovering biophysical mechanisms at the nanoscale, but also of developing third-generation DNA sequencing and DNA mapping technologies, which seek to load and analyze complex genomic material within nanoscale spaces[30, 31, 32, 33, 34].

Despite a flurry of technology development, existing single-molecule approaches to probing biomolecular processes face challenges in simultaneously achieving reproducible

throughput and sensitivity, as well as temporal control and resolution of dynamics and kinetics, over a wide range of reagent and imaging conditions. Retaining structural integrity of complex genomic samples while overcoming several orders of magnitude of applied confinement during sample-loading presents an additional challenge [35, 36].

Prior single-molecule microscopy of molecular interactions has typically used surface-immobilized or tethered DNA molecules for convenient data collection and analysis. While Total Internal Reflection Fluorescence (TIRF) microscopy has enabled exquisite visualization of interactions between surface-immobilized and freely diffusing molecules, providing important biophysical insights[37], these measurements can be limited by surface and tethering effects, as well as low accessible concentrations and short per-molecule trajectories of the diffusing species.

Furthermore, a range of micro- and nanofluidic fabrication approaches have been developed to achieve sub–persistence-length confinement of DNA and other polymers. By extending DNA polymers in nanochannels, genomic features may be mapped to position along the DNA length[38, 39], of interest to advancing sequencing and mapping applications. Visualizing interactions between extended DNA and biomolecules allows sequence-specific processes to be probed and understood, such as targeted labeling[40], binding[41], or cleavage[42]. Existing nanofluidic approaches typically load DNA molecules into nanochannels from the side using electrophoresis for in-situ visualization[43, 44, 39, 45, 46].

PDMS-based microfluidics have provided complementary approaches for important proof-of-principle studies, ranging from drug discovery to biomarker detection to genomic analysis platforms[47]. PDMS allows for rapid prototyping and production of single-experiment devices, often required because PDMS is a porous material and risks contamination with re-use. Work by Zhang et al, in particular, showed one method for interfacing reagents with confined DNA in a fluidic PDMS device[48, 49, 50]. Their fabrication methods allowed average nanochannel cross-sectional diameter down to 200 nm.

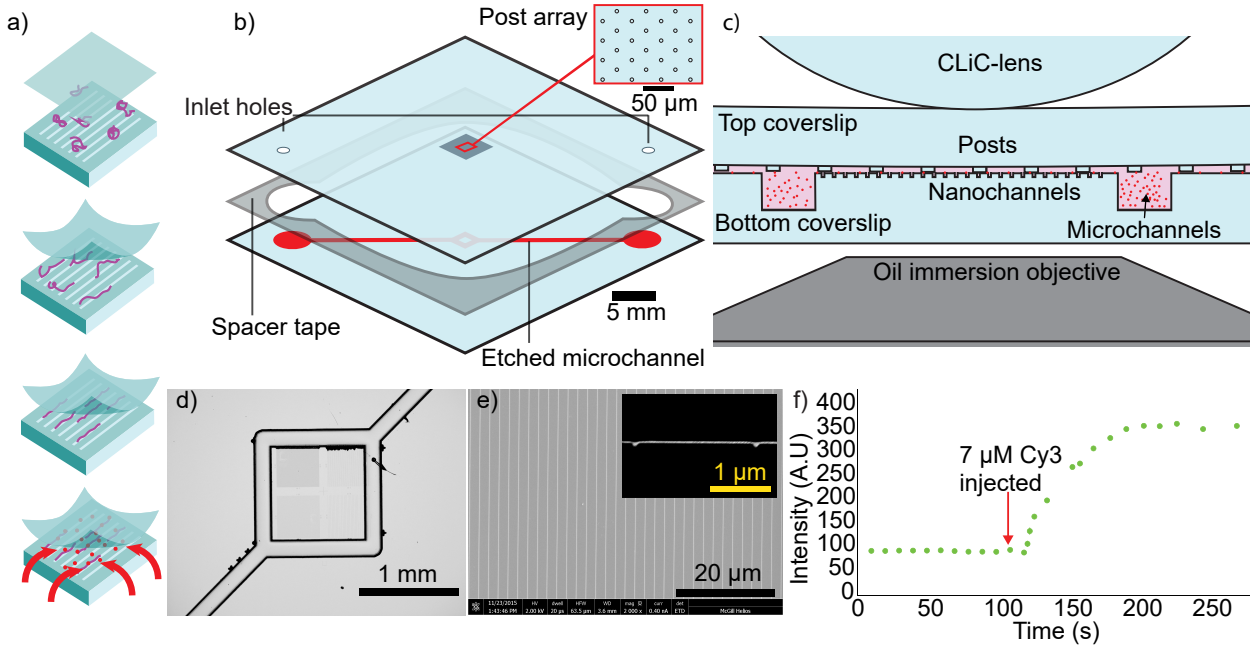

Figure 2.1: Nanofluidic device (not to scale unless otherwise noted). **a)** Schematic of DNA confinement and reagent introduction process. Top device surface is deformed downward, loading the sample into a gradually thinner slit. When the slit height approaches the 50-nm DNA persistence length, DNA enter and extend along embedded, open-face 50-nm nanogrooves. Subsequent reagents can be introduced from the surrounding microchannel. **b)** Schematic of micro- and nanofluidic flow cell. An embedded microchannel in the bottom surface (30-micron-deep, 200-micron-wide) encircles and delivers reagents to the central nanogroove array, where DNA is extended and trapped. A post array on the top coverslip creates a homogeneous slit in which reagents can diffuse. Holes sandblasted into the top coverslip enable sample insertion and removal. Top and bottom coverslip surfaces are held together by a 10-micron-thick double-sided adhesive with a laser-cut flow channel. **c)** Side-view schematic of device. **d)** Optical microscope image of the central nanochannel array and encircling microchannel. **e)** SEM image of nanochannel array (inset: nanochannel cross-section). **f)** Fluorescent intensity of the central CLiC region after introduction of Cy3 fluorescent dye, excited by a 532-nm laser (82 $\times$ 82 microns field of view) and indicated by the red arrow. A lag on the order of 10 seconds corresponds to the time it takes for the dye to diffuse into the central field of view after insertion.

In this work, we introduce a glass-based platform for controlling and visualizing biopolymer and biomolecular interactions in customizable, dynamically adjustable nanoscale environments (Fig. 5.1). This platform enables separate control over loading and formatting biopolymer conformations, and introducing reagent biomolecules. Importantly, it decouples challenges in loading samples from challenges in exchanging reagents, which facilitates studying multi-step biophysical processes in nanoconfined spaces. The glass-based format is compatible with scalable wafer-based fabrication and a wide range of applications.

To illustrate, an experiment performed using this nanofluidic platform can proceed via a two-step process: 1.) the microfluidic chamber roof is deformed downwards, which squeezes biopolymers within the open-face, embedded nanotopographies, from the top. This top-loading approach leverages the principle of "Convex Lens-induced Confinement" (CLiC) imaging, which has previously been used to confine molecules for passive, extended observation within a nanoscale slit[25, 51] as well as within nanogrooves, where deflection off of chamber walls results in high extension[52, 26, 28]. While in prior work the deformed roof was pressed into contact with the floor, creating a curved chamber geometry over the extended imaging region resulting in a confinement-gradient and sample-depletion, in this work, a sparse array of posts has been fabricated to establish stable, precise, and homogeneous confinement across the imaging region. 2.) The microfluidic device enables reagent introduction within the nanofludic imaging region by way of a deep, encircling microchannel embedded in the chamber floor. Reagents subsequently diffuse from the microchannel into the nanofludic imaging region through the fixed-height slit.

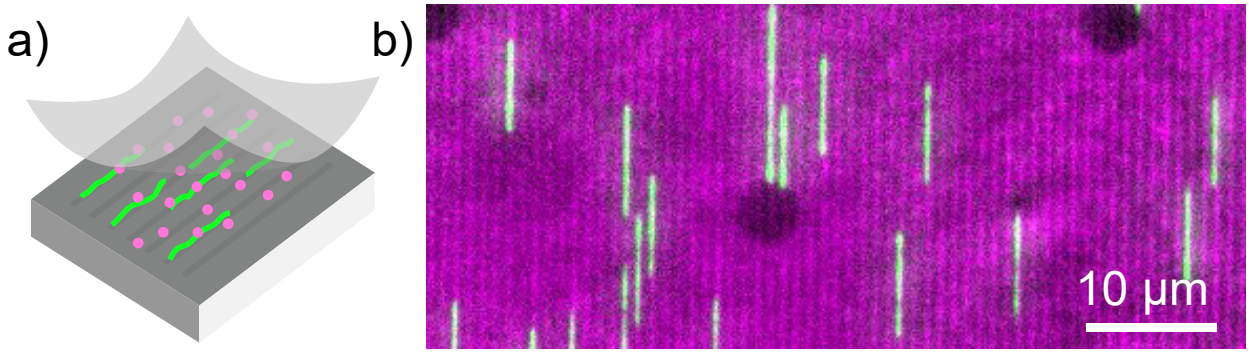

Figure 2.2: DNA confinement in the device. **a)** Schematic of DNA polymers (green) confined to nanochannels in a buffer containing a fluorescent dye (magenta). **b)** False-color fluorescent image of confined YOYO-1–stained λ-phage DNA (green) in buffer containing Cy5 dye (magenta), used to image the extruded posts (dark circles). The sample is illuminated with 488- and 647-nm excitation lasers, for YOYO-1 and Cy5 respectively; this image superimposes spectrally separate fluorescence images.

2.3 Experimental section

As shown in Figure 5.1, the nanofluidic device uses a flow-cell formed between two coverslips which contain embedded micro- and nano-topographies, defined by standard semiconductor fabrication techniques. The top flow-cell surface contains a sparse array of post extrusions (20-100 nm tall) which, by coming into contact with the bottom surface, creates a nanoslit through which reagents can be exchanged. The bottom chamber surface contains linear embedded nanogrooves, typically 40–50 nm deep, into which DNA polymers can be introduced as the CLiC-lens is lowered (Fig. 2.2). The total vertical confinement applied to the nanogroove-confined biopolymers, when using 20-nm posts, is approximately 60 to 70 nm, a regime in which loops and folds in the DNA conformation are highly suppressed[53]. Further, surface-passivation agents such as polyvinyl pyrrolidone (PVP) will typically coat device walls (with a thickness estimated to be around the hydrodynamic radius, 5.6 nm for 55 kDa PVP[54]), further reducing the effective confinement experienced by the DNA.

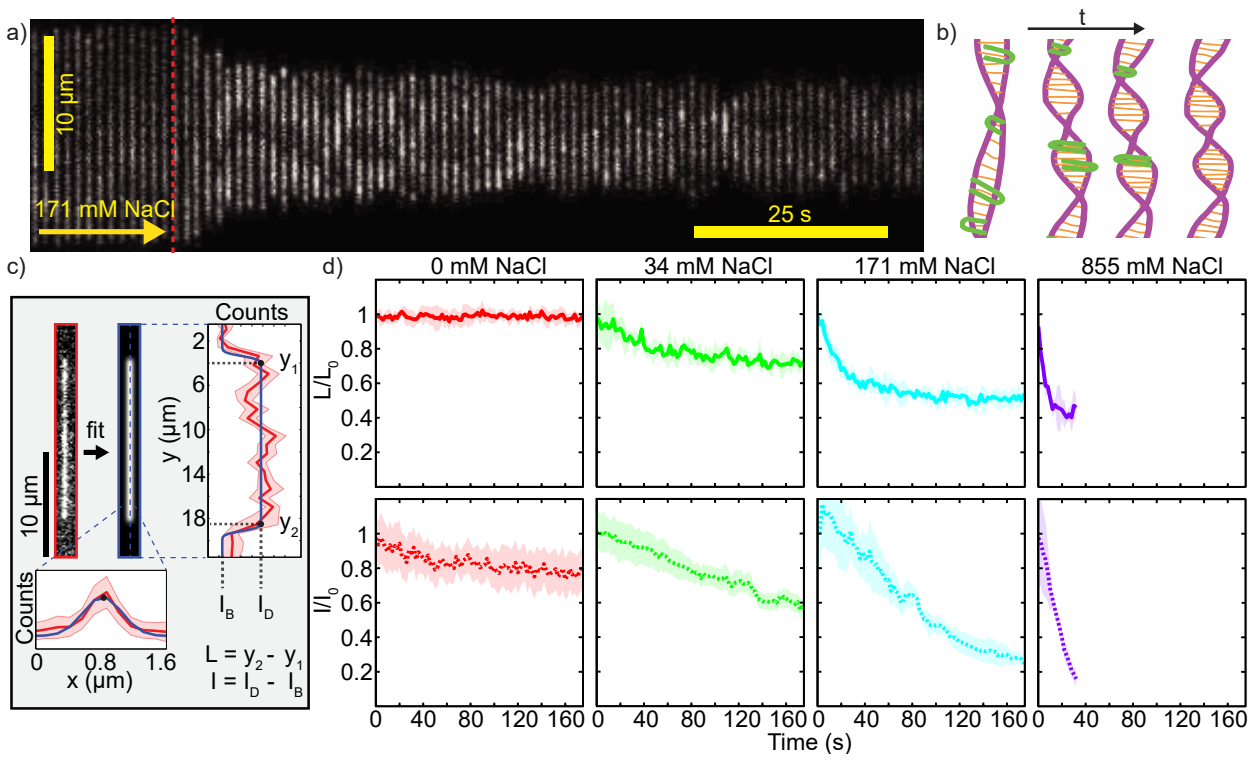

Figure 2.3: DNA extension and intensity in response to increasing ionic strength. **a)** Kymogram of a confined YOYO-1–stained λ DNA molecule in response to buffer exchange from 0 to 171 mM added NaCl. The red dashed line indicates the time of buffer injection. **b)** Schematic of proposed mechanism of DNA extension and intensity changes under increased ionic strength. The negative charges along the backbone are screened, decreasing persistence length. At the same time, the intercalated and electrostatically-coupled YOYO-1 molecules (green) dissociate. **c)** Fitting procedure for extracting DNA length and fluorescent intensity from experimental data. **d)** Normalized length and intensity of 5–10 DNA molecules (in each instance from a single experiment) for a control with no added salt, as well as three experiments with salt concentrations increasing from 0 to 34, 171, and 855 mM NaCl. The shaded regions indicate the standard deviation. I_0 and L_0 are measured per DNA molecule just before introduction of a new buffer solution. Introducing the 855 mM NaCl buffer causes the DNA intensity to drop to background within 40 seconds, after which the trace is not shown.

For inserting reagents, a 30-μm-deep microchannel is embedded in the chamber floor, encircling the nanogroove array and imaging region. Since the hydraulic resistance experienced by the inserted fluid is inversely-proportional to the cube of the applied confinement[55], introducing reagents through the microchannel results in low disturbance to confined DNA. Importantly, this device decouples the initial confinement of DNA from their subsequent interaction with reagents, proteins and other biological molecules, allowing subsequent interaction-induced dynamics to be visualized and influenced by the customized nanoconfinement. More detail on fabrication and experimental procedure is provided in the appendix. The following experiments each report results from a single experiment's single field of view, for each reagent introduced, illustrating ease of use and potential for high throughput.

2.4 Results and discussion

2.4.1 Dynamic response of YOYO-1-DNA to changes in ionic strength

Here, we visualize the dynamic effect of increasing the ionic strength of solution on DNA–YOYO-1 complexes confined within nanogrooves, and address outstanding questions on how YOYO-1 influences DNA length and stiffness. The nature of YOYO-1 binding to DNA molecules remains of keen interest to the nanofluidics field, with differing view points among researchers[56, 57, 58, 59, 60, 61, 62], especially given its frequent use as a stain.

It is generally understood that fluorescing YOYO-1 dye is electrostatically coupled to the negatively charged backbone of DNA, and its bis-intercalating fluorescent ring structures interleave between the π-stacked bases. More interestingly, recent experiments have suggested a complex kinetic picture. Multiple modalities of YOYO-DNA binding have been proposed, ranging from "groove-binding" to "intercalating" modes, with different strengths of association[63, 58].

Because YOYO-1 dye molecules are thought to interleave within the DNA backbone in the "intercalating mode", one may expect YOYO-1-DNA intercalation to contribute to an increase in persistence length. However, reported measurements are divided on the effect of YOYO-1 on persistence length[56]. While some experiments report an increase in persistence length proportional to overall increase in contour length as a function of YOYO-1 addition [64, 65], other experiments suggest that the persistence length remains unchanged or decreases with YOYO-1[56, 62].

As the association of YOYO-1 dye with DNA is mediated by interaction of four positive charges on the dye with the negatively charged DNA backbone, it is possible to probe this interaction by adjusting the ionic strength. Prior measurements of length have been performed in side-loaded nano-slits and nanochannels, following incubation in buffer solutions of desired ionic strengths[66, 65, 67]. This approach obscures dynamic information which could be made available by visualizing molecules during the buffer exchange.

Additionally, prior work has not directly quantified the dynamic change in DNA intensity which we report in this work. Dynamic imaging during solution exchange offers the ability to directly correlate the change in YOYO-1 fluorescence, and hence YOYO-1 binding with DNA, with the change in DNA length. Integrated intensity along the molecules is expected to scale linearly with the number of bound YOYO-1 at a ratio below approximately one dye per 10 basepairs[68], and dye molecules that unbind from DNA emit over 1000 times less fluorescence.

Here, we leverage the capabilities of our nanofluidic platform to measure dynamic changes in length and integrated intensity of single DNA molecules introduced to buffers of increasing ionic strength, and to distinguish between two qualitatively different, salt-induced DNA dynamics, which occur on different timescales: 1.) ionic screening of the polymer and 2.) de-intercalation of YOYO-1 from the polymer backbone (Fig. 2.3 a,b). Specifically, we perform time-resolved measurements of DNA length and integrated intensity as a function of ionic strength of solution. Fig. 2.3c delineates fluorescent images

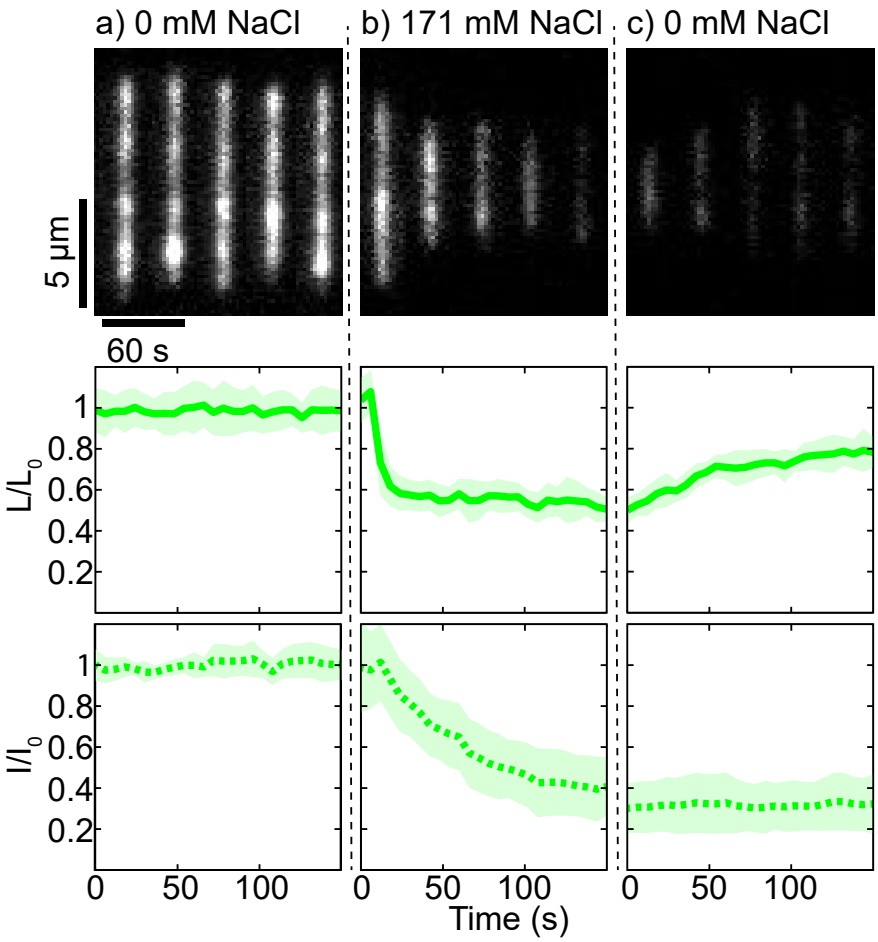

Figure 2.4: DNA extension and fluorescence intensity in response to salt-induced conformational changes. **a)** DNA are confined in nanogrooves in the absence of NaCl. **b)** 171 mM NaCl is introduced via the microchannel. **c)** The NaCl-containing buffer is again replaced with an NaCl-free buffer introduced through the microchannel. Kymographs are corrected for center of mass. Length and intensity measures (following procedures in Fig. 2.3) represent averages of 5–10 molecules, with the shaded region indicating standard deviation.

of DNA molecules during buffer exchange, which we fit for the DNA extension L and integrated intensity I as functions of time, using procedures established in Berard *et al*[26]. To simplify, quantitative results are shown for DNA molecules which do not overlap with other molecules, do not photocleave during imaging and do not escape the field of view. It is possible that excluding photocleaved molecules effects the measured sample, as DNA

with less fluorescent dye associated may be less likely to photocleave. However, the overall photocleavage rate during the course of these experiments was extremely low, so we assume that this effect is negligible. Additionally, we find that all DNA molecules seem to drift equally, so the molecules remaining within the frame of view are not behaving differently from ones that drift out of it. We observe DNA length to decrease when a higher–ionic-strength buffer is introduced and to stabilize to a final value within $\sim$80 s (Fig. 2.3d), commensurate with diffusion times for these molecules over a few hundred microns from the microchannel. This fractional length change is in agreement with other published results[65] but the time-resolved behaviour is a new contribution.

We observe the DNA length to reach a final value well before the YOYO-1 binding equilibrates, as indicated by the DNA brightness continuing to change. The data suggests that YOYO-1 molecules take longer to dissociate from the DNA backbone, potentially due to complex, multi-step unbinding modalities, compared to the timescale for the polymer length to reduce due to increased ionic concentration.

That there is a latter period wherein YOYO-1 brightness decreases while the length doesn't change indicates that there are fluorescing modes of binding that do not contribute to DNA mechanical properties, including persistence length. One potential explanation could be that during the unbinding process, the YOYO-1 dye transitions between the proposed "intercalating" vs. "groove-binding" modes, but continues to exhibit high fluorescence in "groove-binding" modes without contributing the contour length.

We perform additional experiments to demonstrate reversibility and to control for the potential impact of photobleaching during microscopy experiments. Using a longer laser shutter time (300 ms between frames, during which the molecules are not illuminated) we reduce photobleaching effects to negligible levels over the time frame of the experiment (Fig. 2.4a). Buffer containing 171 mM NaCl was introduced (Fig. 2.4b) and then replaced with 0 mM NaCl buffer (Fig. 2.4c). Suppressing photobleaching clarifies the contrast in timescales over which length and intensity vary, which, respectively, are from less than

50 s to over 150 s.

Figure 4 delineates recovery of extension but not intensity, consistent with the release of the dye. The extension recovers only to about 80% of its initial value, for a few potential reasons. The non-recovered extension could be due to depletion of dye molecules, or to residual salt in the chamber, after the second buffer exchange. In quantitatively assessing these options, we used the established measurement of the contour-length contribution of intercalated YOYO-1 dye, reported as 0.5 nm per YOYO-1 molecule[56]. Our staining ratio of 1 dye molecule per 10 bp (natively 0.33 nm per base pair) corresponds to a 15% increase in contour length. If we take from the fluorescence measurement that the DNA has lost between 60 and 70% of its bound dye, then the lost dye could only account for 10% of the extension. The other 10% of unrecovered extension indicates some other effect on DNA nanochannel extension. One possibility is that NaCl has been shown to decrease the negative surface charge in glass nanochannels[69] which in turn has been shown to affect the extension of nano-confined DNA[70]. Such surface charge modification could account for lower polymer confinement in this application; this could be further suppressed and explored in future applications by varying surface-passivation agents. In summary, we have successfully demonstrated two dynamic effects of ionic strength on YOYO-1-complexed DNA, probing open questions on the influence of salt and intercalating dyes upon DNA properties.

2.4.2 DNA compaction with the cationic surfactant CTMA

Further to this exploration, our technology facilitates study of DNA compaction in a wide range of contexts, as well as study of reactions with enzymes and proteins sensitive to DNA topology. Control of DNA compaction has important consequences in DNA packing, replication and transcription. The human genome, for example, would correspond to two meters (end-to-end) of naked native DNA, but is stored in a cell nucleus about 10 microns in diameter, representing a reduction in scale by several orders of magnitude. There

is much interest in how this transition comes about, and many methods have been applied to recreate and visualize DNA compaction *in vitro* with controlled, few-component systems[71].

Previous work has revealed DNA compaction processes in specific confined and crowded environments, for instance environments in which the DNA is initially stretched electrophoretically [49]. Long-time compaction dynamics of DNA with a nucleoid-structuring protein have also been observed [50]. It has been hypothesized that despite a variety of approaches to achieving DNA condensation—surfactants, divalent salts, molecular crowding—the condensed conformation is "universal", a tightly coiled toroid[72].

Here, we visualize dynamic, temporally controlled compaction of DNA polymers immersed in a cationic surfactant solution. For these studies, we use the surfactant cetyl trimethyl ammonium chloride (CTMA), which has a positive head group and a long hydrophobic tail. The positive charges are hypothesized to bind along the length of the DNA and cause the DNA to condense and eventually precipitate[73]. We explore the dynamics of this condensation transition with single-molecule resolution to establish a transition timescale.

To suppress interactions with the walls of the nano-channels, which require more care in these experiments to minimize non-specific adsorption, we treat the glass with the fluorinated silane 1H,1H,2H,2H- perfluorooctyldimethylchlorsilane (FOCS). This creates a hydrophobic, inert surface-layer, complemented by an in-situ coating with polyvinyl pyrrolidone (PVP). CTMA and YOYO-1 both associate to DNA via ionic interactions; to avoid the effect of this competition in these experiments, we labeled the λ-phage DNA covalently with Cy3 moieties. Photobleaching was suppressed by an enzymatic oxygen scavenging system. The compaction buffer contains 92 mM CTMA.

After introduction of the CTMA buffer, we visualize a compaction transition in exposed DNA molecules. The reaction progresses toward the center of the chamber from the microchannel area, representing the diffusing front of the CTMA solution (Fig. 2.5). As

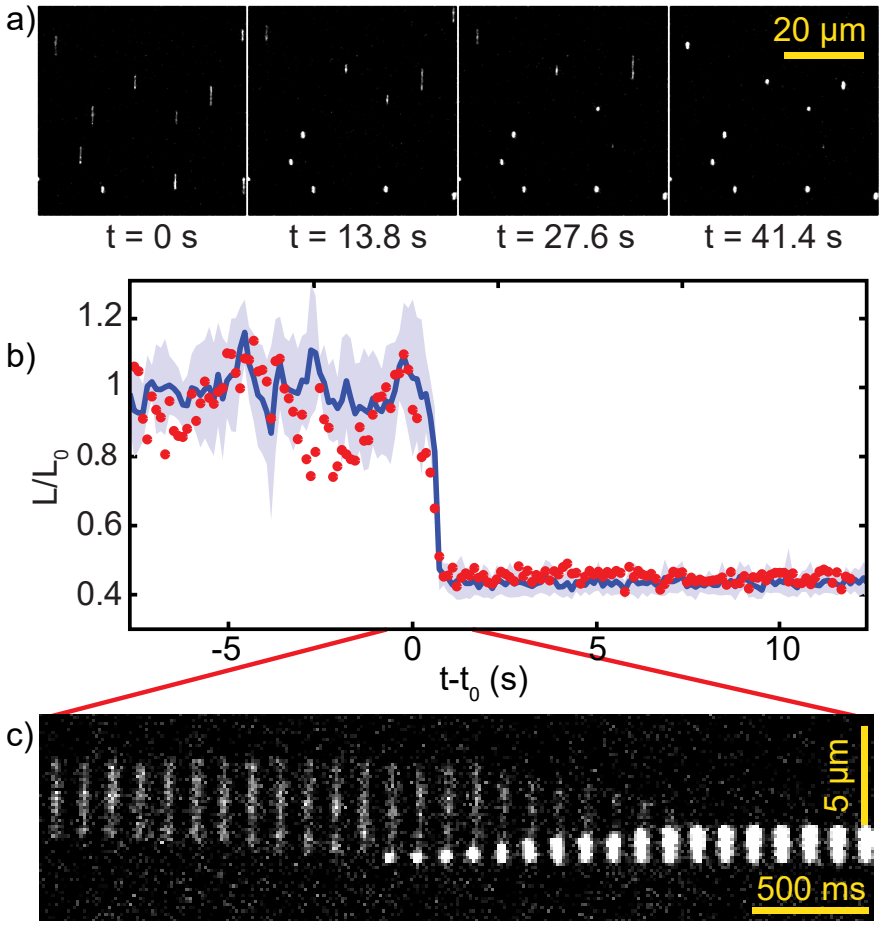

Figure 2.5: λ-phage DNA extension and condensation in response to CTMA, a cationic surfactant. **a)** Images of confined Cy3-labeled DNA in nanochannels acquired after introduction of CTMA. Condensation of DNA proceeds with the diffusion front of CTMA. **b)** Mean fractional extension of 7 DNA molecules undergoing compaction. Trajectories have been aligned to maximize correlation of the signals, where t_0 indicates initiation of the compaction for each molecule. Shaded region indicates the standard deviation. Red dots indicate the trajectory of a single representative molecule. **c)** Kymogram of a representative DNA molecule (shown by red dots) through the compaction transition. Compaction nucleates at one end of the DNA, oriented towards the nearest microchannel.

the CTMA solution approaches the DNA polymers, we visualize the DNA being pulled toward the solution interface, and for compaction to proceed along the polymer length. At the end of the timecourse, the polymer finally appears adsorbed onto the chamber

walls. The "compacted state" is empirically characterized as a 2.5-fold increase in local intensity as well as decrease in polymer length to ∼40% of its initial value. A consistent feature among measurements of many molecules, the compaction nucleates at the end of the DNA molecule closest to the microchannel and proceeds along the length of the polymer in ∼1.5 s. Eventually, the compacted molecules adsorb onto the surface and do not exhibit resolvable fluctuations in intensity or length (Fig. 2.5b,c). In the compacted state, the DNA are still confined by the nanogroove and top surfaces: rather than compacting into a spherical globule, as we observe in unconfined experiments, we observe a collapse into characteristic "chain of smaller globules" aligned with the highly confined nanogroove. We cannot rule out that this could be due to polymers adsorbing before compaction is complete. However, the 600-nm size of chained globules is consistent among observed molecules. Quantitatively, it is interesting to point out that this in-situ compaction occurs on a larger length scale than the λ-phage virus packing its DNA in its 60-nm capsid[74]. This experiment motivates and facilitates further study of a wide range DNA compaction processes as a function of nanoscale confinement, surfactant tail length, and reagent conditions which have otherwise remained out of reach.

2.4.3 DNA cleavage via restriction enzymes

Next, we explore a third nanofluidic application corresponding to the function of restriction enzymes in nanoscale environments. Restriction enzymes are routinely used to cut DNA at specific sites, with a wide range of applications in biochemical processes[75]. Previous work has demonstrated the use of restriction enzymes in optically mapping genetic material fixed to agarose gels or glass[76], as well as in nanochannels[77]. Restriction mapping offers a way to determine long-range structure in genetic material (over many kbp), highlighting, for example, large transpositions which may be difficult to observe in state-of-the-art basepair-level sequencing techniques[78]. Restriction mapping in nanochannels has the benefit of collecting sufficient mapping information from a sin-

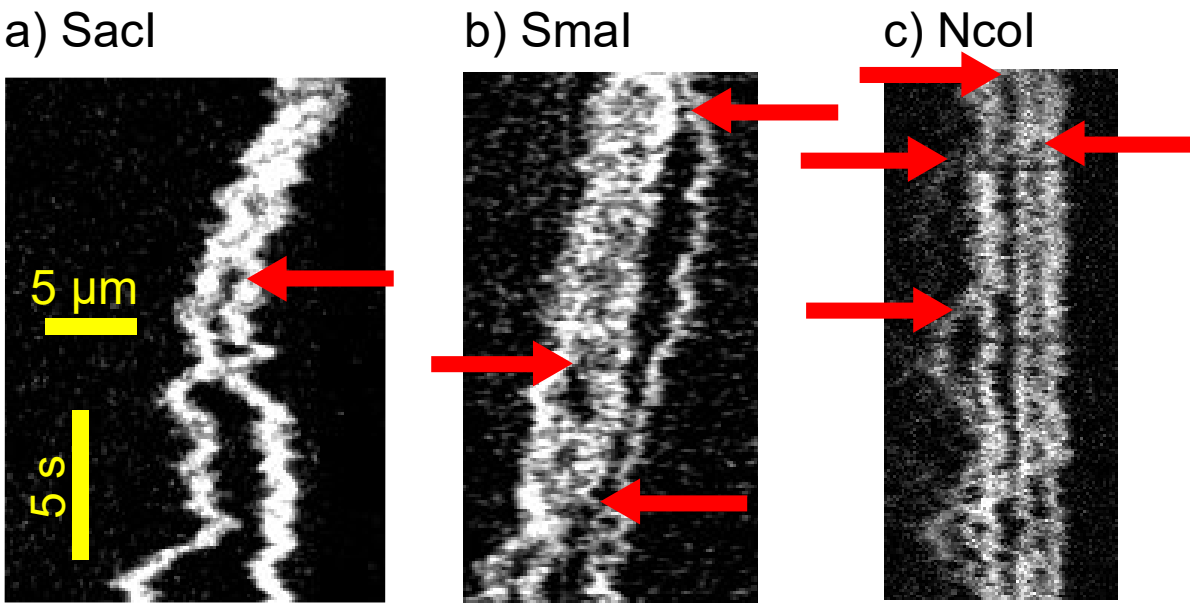

Figure 2.6: Kymographs of YOYO-1 stained λ-phage DNA being digested by the restriction enzymes **a)** SacI (with 100-nm posts), **b)** SmaI (with 40-nm posts), and **c)** NcoI (with 5-nm posts) after introduction of buffer containing 1 mM $MgCl_2$.

gle molecule, as the ensemble-average of conformational fluctuations can be determined from a video of a diffusing polymer. In contrast, samples fixed to a surface require averaging over many molecules[76, 77], as each molecule is in one conformation.

We investigated how our technology could be applied to study temporally controlled single-molecule restriction mapping. The separation of steps between 1.) extending DNA and 2.) introducing the activating reagent, is achieved by first lowering the CLiC-lens to confine DNA in the nanogrooves and subsequently introducing magnesium ions through the microchannel. Unlike previous technology, our device does not require use of electrodes to electrophoretically load DNA or magnesium ions[77]. We demonstrate restriction of DNA molecules that are confined in nano-geometries smaller than previously reported, using 100, 40, and 5-nm posts.

Using this approach, we are able to visualize reactions of more than 30 molecules in one field of view. As a demonstration of use of this method at high levels of confinement,

we present direct visualization of enzymatic activity, using 3 different post heights and 3 restriction enzymes acting on λ-phage DNA: SacI (producing two four-base 3' overhangs at 24772 and 25877), SmaI (three blunt ends at 19399, 31619, and 39890), and NcoI (four four-base 5' overhangs at 19329, 23901, 27868, and 44248). For SacI, SmaI, NcoI and we expect to resolve 1, 3, 4 cuts (labeled by red arrows in Fig. 2.6) corresponding to fragments larger than about 1 kbp, respectively. As in prior work[77], cuts associated with smaller fragments are not shown.

We visualize SacI and SmaI, and NcoI reactions using chambers with 100, 40 and 5-nm posts, respectively. The chamber was pre-passivated with a 10% 55 kDa PVP solution, as magnesium is a divalent cation that can cause DNA to adsorb to glass. All restriction experiment buffers contained 20 mM Tris-HCl (pH 8), 50 mM potassium chloride, 1 mM DTT, 10% 55kDa PVP and 3% BME. DNA was immersed in buffer with restriction enzymes (NEB) at concentrations of 2,000 units/mL for SacI and SmaI and 1,000 units/mL for NcoI, where a unit is defined as the amount of enzyme required to digest 1 μg of λ-phage DNA in 1 hr at optimal temperature.

Experiments performed in the absence of magnesium or enzyme did not show cleavage during the duration of the experiment, which was over 5 minutes. After introduction of buffer containing 1 mM $MgCl_2$, most cleavage events occurred within two minutes. As expected, experiments with SacI, SmaI, and NcoI exhibited 1, 3 and 4 cuts with resolvable fragments, respectively (Fig. 2.6). Our results demonstrate the functionality of a suite of enzymes in the presented nanoconfined environments. We see restriction enzyme activity with posts as small as 5 nm and no discernable effect of post height on activity for the presented experimental conditions.

2.5 Conclusions

In summary, this work establishes a new, glass-based nanofluidic platform to control and visualize reactions in nanoscale spaces. It leverages the principle of CLiC imaging, which allows for continuously loading and extending biomolecules within customized nanoscale environments. This work introduces temporal control of reagent insertion within a CLiC-nanoslit, subsequent to formatting polymer conformations in embedded nanostructures, by introducing new features, including a microchannel and a nanopost array, into the device design. Because embedded nanotopographies are fabricated on thin coverslips compatible with high-NA oil-immersion objectives, our technology provides real-time visualization of reaction dynamics with down to single-fluorophore sensitivity[28].

The glass-based design is compatible with scalable, wafer-based fabrication processes, especially once in a miniature format, which is a subject of current research. Of great interest to the biotechnology sector, this platform could be applied to visualize, diagnose and optimize a broad range of enzymatic reactions in real time, such as ligation and labeling reaction steps used in genomic and other diagnostic platforms. In the field of DNA nanotechnology, it could be used to visualize and influence both synthesis and degradation of DNA nanostructures, providing new insights into the structural dependencies of these processes.

Beyond solution-based fluorescence microscopy applications, which provide visualization of dynamics but are limited in spatial resolution, this platform could be used to format and deposit biomolecules on surfaces, which can subsequently be recovered for higher-resolution analysis. For instance, deposition of molecular complexes onto specific surfaces could be chemically initiated after dynamics of the same molecules are observed in solution, which is a subject of current research. Large numbers of deposited complexes, with conformations influenced by the nanotopography, could be analyzed using high-resolution systems such as atomic force microscopy (AFM) or forms of electron microscopy (EM) following device-disassembly.

Overall, this nanofluidic platform can be applied to explore and manipulate a wide range of fascinating biophysical interactions of interest to biological, biotechnological, biophysical, chemical, and materials science research communities, in customized nanoscale environments.

Chapter 3

Linearizing and depositing DNA molecules for high-resolution visualization

The preceding manuscript presented a device that could see wide use in biomolecular studies. The glass surfaces are smooth, non-porous, and inert to many chemicals. Additionally, as seen above, they can be treated with silanes and other chemicals to change their properties, making a broad range of reagents and solutions compatible. Nanotopographies are customized to different purposes, as seen in our prior work, wherein DNA confined to closed circles are ligated by enzymatic action, a topography not possible in conventional nanochannel devices which require and inlet and outlet.

Another unique benefit of our device, as demonstrated in this chapter, is the reversibility of the nanoconfinement. Because the confining roof is held in place by a lowered push-lens, the lens can be lifted in order to retrieve molecules that have been confined in reactions. In particular, we introduce a bifunctional linker, APTES, that binds DNA to exposed hydroxyl groups on the clean silica surface. Modification of the bottom nanotopography surface with a fluorinated silane renders those confining surfaces inert - thusly,

the user can select the surface that DNA binds to. Lifting the push lens, removing the flow cell from the CLiC device, and dissolving the acetone allows high-yield retrieval of templated, extended DNA. This technique can be extended to SEM and TEM-compatible membranes with silica or similarly treatable surfaces, such as silicon nitride. Contributions to this work are listed in the appendix.

3.1 Abstract

We present a new method for templating gently extended DNA onto a selected surface using convex lens-induced confinement. We report visualizing extended DNA binding to a hydroxylized silicate surface using the silane APTES, where binding can be limited to this surface by treating the glass with the inert silane FOCS prior to confinement. We report high yield of intact, bound DNA following disassembly of the flow chamber, indicating that DNA can be then transferred to higher resolution microscopy tools such as AFM or TEM.

3.2 Introduction

As genomic sequencing techniques have advanced in the past decade, there is much interest in expanding the available tools. The most popular current sequencing method, Illumina dye sequencing, requires making many copies of much smaller segments of the DNA of interest. The amplification required can skew the sequenced material towards errors made early in the process. Additionally, Illumina dye sequencing faces computational challenges in reconstructing long sequences from the short individual reads, and additionally may not detect rare mutations, inverted subsequences, long range transpositions, or copy number variations. Single molecule methods are also being developed which increase the length of a single read: however, these suffer from high noise levels in

indirect measurement which result in higher error during sequence analysis [79].

A method for electron microscope sequencing can cut down significantly on errors due to reconstructing reads from small segments reduce computation requirements, including time, by simply looking at the bases to read them off one by one. Examining long sequences from single DNA strands also facilitates cheaper and faster *de novo* genome assembly. Additionally, examination with high resolution microscopy allows open-ended exploration of biomolecules, including DNA-protein complexes [80].

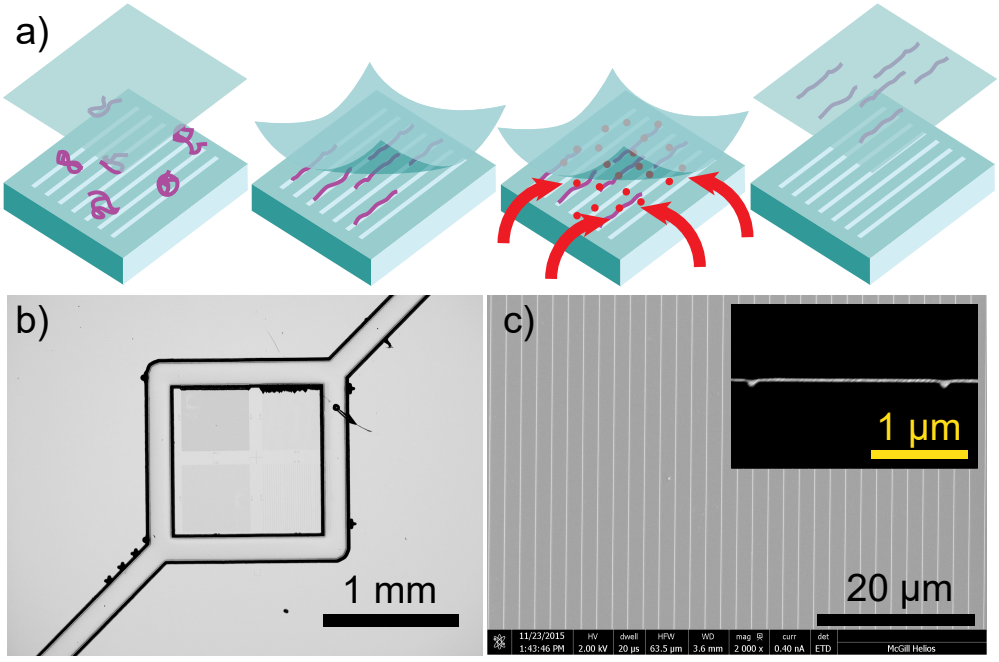

Figure 3.1: DNA confinement and transfer device. **a)** Schematic of device operation. DNA in bulk solution is gently confined from the top until extension in 50-nm grooves is entropically favored. The DNA can then be treated from an encircling microchannel with a binding silane. The top coverslip can be lifted with high yield of bound DNA. **b)** Bright field image of device nanogooves and microchannel. **c)** SEM image of a nanogroove array, with example channel profiles inset.

One limiting complication of electron microscopy techniques is the challenge presented by requirements on sample preparation. The DNA must be adhered to the surface of a clean, nanometers-thin membrane, to suppress any fluctuation of DNA during

measurement and to allow passage of electrons through the sample to the detector. Additionally, to facilitate rapid analysis, the molecules ought to be sufficiently stretched to suppress looping of the polymer. Methods to prepare DNA for such analysis include embedding molecules stretched by electrospinning in polymer nanofibers [81] and molecular combing, which has been demonstrated on membranes as thin as graphene [82]. These methods often lack control required to linearize an array of molecules with sufficient density for easy analysis at high resolution.

A precise and well-characterized method of stretching DNA uses physical confinement. The DNA is brought into a nanochannel of confinement dimensions around 50 nm, the persistence length, which causes the polymer to elongate to as much as 90% of its total contour length (depending on confinement dimension) as it deflects off of the solid confining surfaces [31]. However, integrating this technology directly with TEM is difficult, as this confinement must done in solution and the nanochannel in conventional devices is surrounded by tens of microns of material preventing electron transit.

We report a new method of linearizing long DNA molecules and depositing them on a selected surface using convex lens induced confinement (CLiC), which allows high-yield retrieval of extended and deposited molecules. CLiC is a simple method of confinement of molecules to nano-scale dimensions[25] that offers a way to gently linearize DNAs by loading DNA from the top of open-face nano-grooves, eliminating loops and allowing confinement of long pieces of DNA without breaking[26]. Further modifications allow chemical treatment of DNA molecules while they are linearized: an array of posts that suppresses the confinement gradient and stabilizes the chamber, and a microchannel that delivers reagents to the nanochannel region. The chamber can be disassembled for transferal to higher resolution microscopes.

3.3 Methods

The device schematic is shown in figure 3.1. A typical device is fabricated on standard glass coverslip surfaces using standard wafer-scale techniques, as described previously[28].

Prior to experiment, the coverslips are cleaned in piranha solution to expose hydroxyl groups and remove organic residues. Once cleaned and subsequently dried under a flow of N_2 gas, laser-cut double-stick tape is fixed to the bottom coverslip (with nanochannels and microchannels) before it is placed in a vacuum dessicator for one hour with 10 microliters of perfluorooctyldimethylchlorosilane (FOCS), which assembles on the hydroxyl groups. Fluorosilanes deposited on such silica surfaces are known to be highly inert [83], and helps prevents DNA or bifunctional linkers from binding onto the surface. The two coverslips are then assembled into a flow cell and brought to the inverted fluorescence microscope, where the assembly is sealed to a fluidic chuck by a silicone rubber gasket.

DNA is stained with YOYO-1 bisintercalating dye at a ratio of 1 dye to 10 basepairs, and is diluted to 50 ng/μL in 0.5x TBE (pH 8) with 3% β-mercaptoethanol (BME, to suppress photobleaching) prior to experiment.

DNA that has been labeled by YOYO-1 fluorescent dye is driven into the unconfined chamber through the microfluidic inlet using positive pressure, and the CLiC lens above the flow cell on a piezo actuator is lowered until the post array is in contact with the bottom coverslip, indicated by darkness in laser interferometry that does not change with further lowering, as well as by observing extension of the DNA polymers in fluorescence using a 488 nm laser line. This confines the DNA to extended conformations, in the nanochannels - the confinement dimension is given by the combination of channel width and depth (50 nm) combined with the height of the post array (20 nm). The CLiC lens is lowered a further 10 to 15 microns to stabilize the chamber during pressure-driven reagent flow.

Once the DNA is confined to the nanochannels, 0.5x TBE buffer containing 3% BME and 1% aminopropyl trimethoxysilane (APTES), mixed just before injecting into the mi-

crofluidic chuck, is introduced through the microchannel. After observing the DNA cease to diffuse in the nanochannel (within 1-5 min), the CLiC lens is lifted and the flow cell may be removed to a bath of acetone, or other solvent, to dissolve the tape adhesive, releasing the surface with adsorbed DNA.

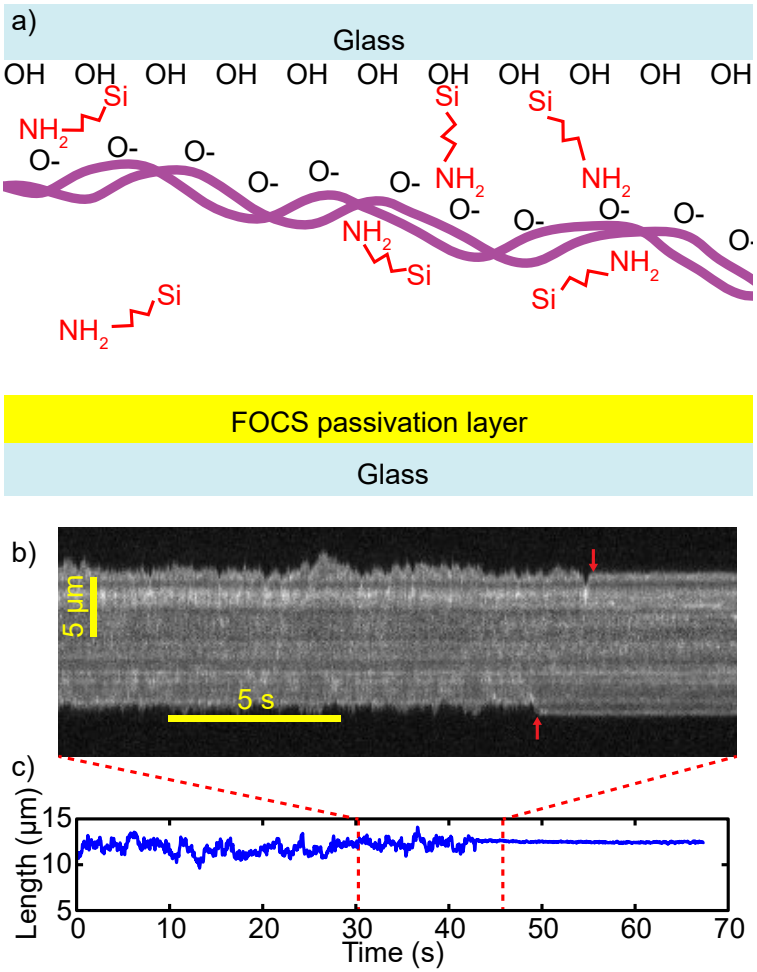

Figure 3.2: DNA surface binding by APTES. **a)** Schematic of DNA adsorbing onto a surface. The bottom surface is previously treated with a hydrophobic, inert silane, FOCS. A second silane, APTES, is then added to solution, which binds to the hydroxyl groups on the top glass surface as well as the negative backbone of the DNA.**b)** Kymograph of DNA in a nanochannel after the introduction of APTES. Red arrows indicate the points where the ends of the DNA stop diffusing, when the DNA has been attached to the glass surface. **c)** Plot of the length of the molecule in b). When the DNA is bound to the surface, the molecule ceases to fluctuate.

3.4 Results and Discussion

Figure 3.2 demonstrates use of the device in binding DNA to glass in the micro- and nano-fluidic device. DNA is initially free to diffuse within the nanochannel, as indicated by the length fluctuations of the polymer. After flowing the solution of APTES, binding is characterized by suppressed end-to-end and diffusive fluctuation, to the point where fluctuation is no longer resolvable (Fig. 3.2b). The binding occurs within minutes of introduction of the buffer and preserves the length of the extended DNA.

After a few more minutes of incubation to ensure that the DNA bound along its entire length, the CLiC lens is raised. The fluorescence signal of the DNA is preserved on the glass surface that has not been treated with FOCS - the FOCS silanes have assembled on the treated surface, leaving a layer of their long fluorinated tails exposed to solution. The APTES has thus bound DNA to the glass with exposed hydroxyl groups only, a process mediated by charge-reversal when the APTES molecules assemble into a two-dimensional organosilane polymer layer on that surface - the amine groups remain protonated up to pH 10 [84, 85]. Because fluorescence of the YOYO-1 dye drops dramatically when unbound to the DNA, we can assume that the DNA is templated on the top surface and not bound to the inert fluorosilane layer on the bottom surface [60].

Following disassembly of the flow cell by dissolving the adhesive in acetone overnight, the bottom coverslip is imaged in fluorescence in air to assess integrity of DNA bound to the surface (Fig. 3.3). The fluorescence image indicates that the DNA remains intact, with the conformation and extension preserved.

3.5 Conclusions

This method provides a new way to linearize DNA on a surface using a highly controlled method. Many existing methods in which a solution containing DNA is dragged across a surface yields uncontrolled coverage. In this method, the deposition process is directly

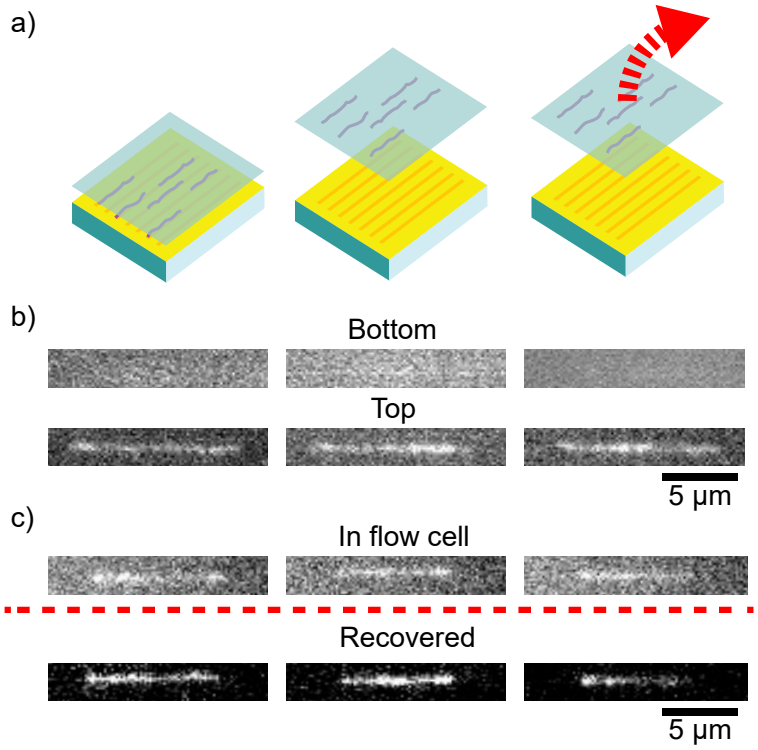

Figure 3.3: Recovery of surface-bound DNA. **a)** Schematic of chamber after lifting CLiC-lens, and removing the top coverslip from the chamber. **b)** Three λ-phage DNA molecules from one experiment which have been bound to the top surface, which has been raised. These images are taken in the flow cell while it is still assembled. Fluorescence on the bottom coverslip is likely due to YOYO-1 dye from solution, there is no discernible DNA shape. **c)** Three DNA molecules which are imaged before and after disassembling the flow cell. The lower signal to noise in the flow cell image is likely due to YOYO-1 in solution, which is washed away in the 'recovered' image, which is imaged in air.

visualized to ensure extension of the molecules and appropriate density on the surface. Additionally, existing methods rely on the speed of the dragging method to control the amount of tangles. Because nanoconfinement in regimes at the scale of the persistence length suppresses all loops, tangles are avoided on the surface. CLiC is the only method to our knowledge that offers this adsorption observed in situ and the ability to recover the surface after depositing extended molecules without loops. The methods reported here can extend to TEM-compatible surfaces, as the silica surface of membrane materials

such as silicon nitride or silicon oxynitride can be treated the same way to expose active hydroxyl groups. Additionally, the open-ended platform can be used for a wide range of studies of protein-DNA complexes under TEM or other high resolution microscopy techniques; the working area of the device is small enough that the whole assembly can be scaled down to 3-mm, the size of TEM-compatible membrane holders.

Chapter 4

Concluding remarks and future directions

The preceding chapters describe a widely useful tool in single-molecule fluorescence experiments. The glass surfaces are non-porous and inert, allowing a large range of compatible reagents. The non-porousness of the glass combined with the dissolvable adhesive means these devices are highly reuseable. Glass structures etched on the glass surface allow new fluidic control, including microfluidic channels to introduce reagents and an array of stand-off posts to allow diffusion of molecules from the microchannel into the nano-confined region. The dissolvable adhesive combined with the demonstrated transfer experiments has the potential to facilitate higher-resolution microscopy on reacted and templated biomolecules. It has been demonstrated that the glass is treatable with silanes as well as in-situ surface modifications to suit different uses.

Using these properties, we have presented a series of experiments as demonstrations. Experiments demonstrate that manipulating ionic strength of the buffering solution can reveal information about DNA conformational dependence on salt as well as an electrostatically intercalated dye. We further show that after introducing a surfactant with a positive head group, we can visualize the dynamic process of compaction. We show

that introduction of restriction enzymes allows visualization of site-specific cleavage activity, which also demonstrated activity of these enzymes in smaller spaces than has been previously shown. Lastly, experiments show that introducing a bifunctional linker, after appropriate surface modifications, allows the user to bind DNA to a silica surface, which could then be transferred to a higher resolution microscope.

In particular, there is great potential in using this device to explore more protein-DNA interactions. The CLiC confinement method provides the unique ability to customize the confinement shape, allowing DNA to be templated in closed circles, as we have demonstrated previously[28]. In that work, long (48.5kbp) DNA molecules confined in circles of the appropriate circumference are ligated into circles. The molecules were incubated with the ligase protein prior to confinement. That work can be extended with the use of microchannels and a post array to study more closely the mechanisms of ligation, and possibly optimize this reaction, which is notoriously hard with such long DNA molecules. Many proteins perform searches along the DNA to find an appropriate sequence for their function. The thin glass allows single-fluorophore detection, meaning that with the proper labeling scheme, these searches can be followed to extract sequence-specific information. Of particular interest in biophysics right now is the proteins responsible for construction of chromatin: condensin and cohesin[86]. Visualizing DNA conformation during reaction with these proteins could provide insight on their activity, which is so far not understood. Finally, DNA that has been templated and complexed with proteins can be bound to the surface for further study under SEM, TEM, or AFM.

The device itself could see improvement in future iterations. The fluidics can be refined to increase throughput, decrease diffusion time, and reduce sample volumes required, by scaling down the device. The 25-mm format currently used is easily obtained as standard coverglasses, and interfaces with many pieces of equipment already in the lab, allowing for quick prototyping of designs, but could be reduced by an order of magnitude. Preliminary experiments have been performed integrating EM-compatible mem-

branes with CLiC, but further work may required to image transferred DNA samples on EM. Current work aims to bring templated DNA to the AFM, which may be able to detect DNA strands on the nanometer-smooth surface.

Chapter 5

Appendix

This document contains further devices fabrication detail, and detail on experimental procedure. Additionally, we present fabrication measurements made on sample devices not shown in the manuscript, and present action of a restriction enzyme at an additional confinement scale.

5.1 Contributions: manuscript 1

The co-authors of the first manuscript are Daniel Berard, Francis Stabile, Marjan Shayegan, Jason S. Leith, and Sabrina R. Leslie. All authors provided significant editorial support during creation and editing of the manuscript. Daniel Berard designed and built the CLiC device, developed fabrication techniques for nanochannels and collaborated on developing fabrication techniques for microchannels, and the post array. Frank Stabile assisted with experiments and device fabrication. Marjan Shayegan took the data for SmaI and NcoI restriction enzyme cleavage. Jason Leith contributed editorial support and theoretical background. Sabrina Leslie guided all research and analysis and contributed editorial support. Gil Henkin wrote the text, took data in the NaCl, CTMA, and SacI experiments, performed device fabrication, did the analysis, and constructed the figures.

The text is reproduced exactly as it is in the submitted manuscript, with references

to video supplementary material removed, and the fabrication and experimental supplementary material moved to the appendix.

A version of this manuscript has been published *Analytical Chemistry*, DOI: 10.1021 / acs.analchem.6b03149.

5.2 Contributions: manuscript 2

The second work, titled "Linearizing and depositing DNA molecules for high-resolution visualization", was also put together with a team of co-authors. Daniel Berard provided device and fabrication support as mentioned above. Frank Stabile performed many of the experiments and developed silanization protocols for the devices. Felipe Guzman and William Glover provided expertise and advised use of the two silane chemicals. Sabrina Leslie guided all research and contributed text. Gil Henkin fabricated devices, collaborated with Frank on experiments, performed analysis, wrote most of the text and made the figures.

This work contains content that will become part of a manuscript.

5.3 Micro/nanofluidic Device Fabrication

For fabricating nanogroove arrays, piranha-cleaned, 170-μm-thick glass wafers (Schott, D263) were patterned with gold alignment marks by standard UV lithography and a lift-off process. After a plasma clean, the coverslips were spincoated with ZEP520A, a positive electron-beam resist, with 20-nm of thermally-evaporated aluminum for a discharge layer. The ZEP is exposed using electron-beam lithography (VB6 UHR EWF; Vistec Lithography) to define nanochannel arrays, with 500-micron $\times$ 50-nanometer nanochannels, spaced by 1–8 microns. The exposed pattern was then developed and etched by RIE for depths of about 50 nanometers.

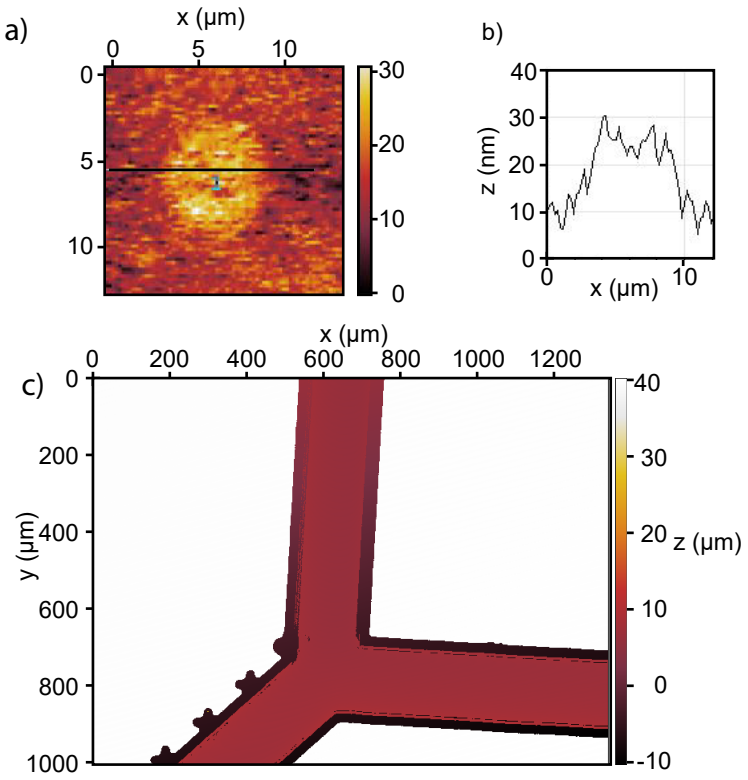

Figure 5.1: Measurements of fabricated features. **a)** A post structure imaged on AFM, with indicated cross section plotted in **b)**. **c)** Optical profiler image of microchannel area, indicating the 30 μm depth.

Microchannels were etched on clean coverslips that were previously patterned with nanochannel arrays, surrounding this central 1.2-mm-square region with a 200-micron-wide, 30-micron-deep microchannel. Sequentially sputtered chromium and gold was etched using UV lithography of S1813 photoresist followed by metal etchants, to create an etch mask for hydrofluoric acid (HF). Immersion in HF subsequently etched the exposed glass to a depth of 30 microns[†]. As shown in Fig. 5.1b, the channel was designed to run between two corners of the coverslip. To enable sample insertion and removal, the entry ends to the channel were positioned below 1-millimeter holes in the top coverslip.

Standard microscopy coverslips (VWR) were used to create the chamber roof, into which inlet holes were sandblasted at the corners. The piranha-cleaned sandblasted cov-

erslips were subsequently patterned with a sparse hexagonal array of 10-μm-wide circles in S1813 resist using UV lithography (EVG620; EV group). The glass was next placed in an RIE chamber for CF_4/CHF_3 etching to a depth of 20 to 100 nm†, leaving the hexagonal array as extrusions on the surface.

Each coverslip underwent a rigorous cleaning procedure before use. Because the flow cells were recovered and re-used between experiments, it was critical for residues to be removed. We treated coverslips in sequential 1% Hellmanex at 50° C, acetone at 50° C, isopropanol at 50° C, and finally 2M KOH in ethanol to remove macroscopic residues, which was followed by a clean in 3:1 sulfuric acid to 30% hydrogren peroxide piranha solution. This approach thoroughly removed any organic contaminants from the surface and exposed hydroxyl groups. Coverslips were rinsed thoroughly with DI water between all steps. Coverslips were then soaked in 100mM KOH, rinsed with DI water, and were ready for use or for further treatments. Since the CLiC microscopy experiments presented in this work require nanoscale surface contact, rigorous cleaning is essential.

5.4 Device and sample preparation

For experiments requiring a particularly inert surface, coverslips were next treated with 1H,1H,2H,2H-perfluorooctyldimethylchlorosilane (FOCS), purchased from Alfa Aesar, prior to use. Coverslips were placed in a vacuum dessicator for one hour with 5–10 μL of FOCS for vapor-phase deposition. The coating could be assessed by examining the shape of a water droplet on the coverslip. A successful coating corresponds to a highly hydrophobic surface.

For most experiments, λ-phage DNA (48.5 kbp, New England Biosciences) was stained in YOYO-1 dye (Life Technologies) to achieve a mixture in solution of 1 dye molecule for every 10 basepairs (16.6 μM for 100 ng/μL DNA). All solutions were diluted in 0.5$\times$ TBE (45mM tris borate, 1mM EDTA; pH 7.8). The mixture was incubated for an hour at 55° C

for uniform dye distribution. For experiments requiring a covalent bond, λ-phage DNA was stained with Cy3 fluorescent dye using a non-enzymatic labeling kit (Mirus). The stained DNA was stored at 4° C at concentration of 100 ng/μL.

Immediately prior to a microscopy experiment, fluorescently-labeled DNA was diluted from 100 to 50 ng/μL in 0.5$\times$ TBE with 3% β-mercaptoethanol (BME) by volume, for YOYO-1–labeled DNA, or 384 μg/mL protocatechuic acid (PCA) and 34 μg/mL protocatechuate-3,4-dioxygenase (PCD), for Cy3-labeled DNA.

5.5 Experimental procedure

The experimental procedure is briefly given in the manuscript chapters above. Here is reproduced the detailed procedure provided in the supplementary information to manuscript 1.

A flow-cell assembled with 10-μm double-sided adhesive (Nitto Denko) was placed on a sample plate above the inverted fluorescence microscope (Nikon Ti-E), and sealed to a microfluidic chuck with a rubber gasket and thumbscrews [51]. The chuck allowed sample loading by applying air pressure at the inlet and outlet holes. The tube holding the CLiC-lens was mounted above the chuck and was lowered by a picomotor (Newport 8392), for coarse control, and piezo actuator (Physik Instrumente P-602.1SL), for fine control, after the flow cell was positioned underneath the lens by a custom translation stage controlled by micrometers. This CLiC device has been previously published [28] The CLiC device and translation stage were positioned relative to an oil immersion objective (CFI Apo TIRF 100x) by an additional translation stage (Physik Instrumente P-545) controlled by a joystick.

To prevent surface adsorption during some experiments, the chamber was washed with 30 μL of 10% 55-kDa polyvinylpyrrolidone (PVP) containing the protocatechuic acid (PCA)/protocatechuate-3,4-dioxygenase (PCD) oxygen scavenging system, and then in-

cubated for 15 minutes before rinsing with 60 μL of 1% 55-kDa PVP [51].

The diluted, fluorescently-labeled DNA was loaded into the chamber and the CLiC-lens was lowered by the piezo device until contact was made between the posts and the bottom coverslip, indicated by imaging the interference pattern of the laser excitation. Glass, once in contact, became characteristically dark and remained dark with further lowering of the CLiC-lens.

After contact was made, the CLiC-lens was typically lowered an additional 10–15 μm to further deform the glass and ensure contact across an extended area [51], as well as to provide stability under pressure during sample-loading. Using a 488-nm laser for YOYO-1 excitation or 532-nm laser for Cy3 excitation, and standard emission filters for these fluorophores' spectra, the DNA extension in nanogrooves was then observed using an EM-CCD camera (Andor iXon Ultra). For different experiments, DNA molecules extended in the nanochannels to 60–90% of their contour length, depending on solution conditions and the applied confinement. Sub–100-nm confinement yielded up to 90% polymer extension, corresponding to the Odijk regime of confinement defined by deflection of the polymer off the nanochannel walls.

Excess solution was removed from the chuck inlet chamber prior to pipetting in subsequent reagents. Reagents were typically diluted in 0.5$\times$ TBE with the appropriate antioxidation reagents (BME or PCA/PCD) to suppress photobleaching. After inserting reagents in the chuck chamber, negative pressure was applied to the chamber via the outlet to load reagent into the microchannels.

For experiments requiring temperature control, a heating collar was placed around the objective, and the a heater installed was directly above the CLiC-lens–tube, as has been previously published [26]. The temperature was set and the CLiC device was allowed to equilibrate before the experiment to prevent thermal expansion from disturbing the confined molecules.

Bibliography

[1] Stefan Haeberle and Roland Zengerle. Microfluidic platforms for lab-on-a-chip applications. *Lab on a Chip*, 7(9):1094, 2007.

[2] Ramon Roman-Roldan, Pedro Bernaola-Galvan, and Jose Oliver. Application of information theory to {DNA} sequence analysis: A review. *Pattern Recognition*, 29(7):1187 – 1194, 1996.

[3] Liang Dai, C. Benjamin Renner, and Patrick S. Doyle. The polymer physics of single dna confined in nanochannels. *Advances in Colloid and Interface Science*, pages –, 2015.

[4] Walter Reisner, Keith J. Morton, Robert Riehn, Yan Mei Wang, Zhaoning Yu, Michael Rosen, James C. Sturm, Stephen Y. Chou, Erwin Frey, and Robert H. Austin. Statics and dynamics of single dna molecules confined in nanochannels. *Phys. Rev. Lett.*, 94:196101, 2005.

[5] T. Siggers and R. Gordan. Protein-DNA binding: complexities and multi-protein codes. *Nucleic Acids Res.*, 42(4):2099–2111, 2013.

[6] Remo Rohs, Xiangshu Jin, Sean M. West, Rohit Joshi, Barry Honig, and Richard S. Mann. Origins of specificity in protein-DNA recognition. *Annu. Rev. Biochem.*, 79(1):233–269, 2010.

[7] Gary D. Stormo and Yue Zhao. Determining the specificity of protein–DNA interactions. *Nat Rev Genet*, 11(11):751–760, 2010.

[8] P Gravesen, J Branebjerg, and O S Jensen. Microfluidics-a review. *Journal of Micromechanics and Microengineering*, 3(4):168, 1993.

[9] Joel Voldman, Martha L. Gray, and Martin A. Schmidt. Microfabrication in biology and medicine. *Annual Review of Biomedical Engineering*, 1(1):401–425, 1999.

[10] P Abgrall and A-M Gu. Lab-on-chip technologies: making a microfluidic network and coupling it into a complete microsystema review. *Journal of Micromechanics and Microengineering*, 17(5):R15, 2007.

[11] Chuanhua Duan, Wei Wang, and Quan Xie. Review article: Fabrication of nanofluidic devices. *Biomicrofluidics*, 7(2), 2013.

[12] Logan R. Myler, Ignacio F. Gallardo, Yi Zhou, Fade Gong, Soo-Hyun Yang, Marc S. Wold, Kyle M. Miller, Tanya T. Paull, and Ilya J. Finkelstein. Single-molecule imaging reveals the mechanism of exo1 regulation by single-stranded dna binding proteins. *Proc. Natl. Acad. Sci. U.S.A.*, 113(9):E1170–E1179, 2016.

[13] Jason Gorman, Feng Wang, Sy Redding, Aaron J. Plys, Teresa Fazio, Shalom Wind, Eric E. Alani, and Eric C. Greene. Single-molecule imaging reveals target-search mechanisms during dna mismatch repair. *Proc. Natl. Acad. Sci. U.S.A.*, 109(45):E3074E3083, 2012.

[14] Anthony L. Forget and Stephen C. Kowalczykowski. Single-molecule imaging of DNA pairing by RecA reveals a three-dimensional homology search. *Nature*, 482(7385):423–427, 2012.

[15] J Christof M Gebhardt, David M Suter, Rahul Roy, Ziqing W Zhao, Alec R Chapman, Srinjan Basu, Tom Maniatis, and X Sunney Xie. Single-molecule imaging of transcription factor binding to DNA in live mammalian cells. *Nature Methods*, 10(5):421–426, 2013.

[16] Robert Riehn, Manchun Lu, Yan-Mei Wang, Shuang Fang Lim, Edward C. Cox, and Robert H. Austin. Restriction mapping in nanofluidic devices. *Proc. Natl. Acad. Sci. U.S.A.*, 102(29):10012–10016, 2005.

[17] Sergey M. Mel'nikov, Vladimir G. Sergeyev, and Kenichi Yoshikawa. Discrete coil-globule transition of large dna induced by cationic surfactant. *J. Am. Chem Soc.*, 117(9):2401–2408, 1995.

[18] Kenichi Yoshikawa, Yuko Yoshikawa, Yoshiyuki Koyama, , and Toshio KanbeŁ. Highly effective compaction of long duplex dna induced by polyethylene glycol with pendant amino groups. *J. Am. Chem. Soc.*, 119(28):6473–6477, 1997.

[19] M. Kojima, K. Kubo, and K. Yoshikawa. Elongation/compaction of giant DNA caused by depletion interaction with a flexible polymer. *J. Chem. Phys*, 124(2):024902, 2006.

[20] Walter Reisner, Jason P. Beech, Niels B. Larsen, Henrik Flyvbjerg, Anders Kristensen, and Jonas O. Tegenfeldt. Nanoconfinement-enhanced conformational response of single DNA molecules to changes in ionic environment. *Phys. Rev. Lett.*, 99(5), 2007.

[21] W. Reisner, N. B. Larsen, A. Silahtaroglu, A. Kristensen, N. Tommerup, J. O. Tegenfeldt, and H. Flyvbjerg. Single-molecule denaturation mapping of DNA in nanofluidic channels. *Proc. Natl. Acad. Sci. U.S.A.*, 107(30):13294–13299, 2010.

[22] M. Xiao, A. Phong, C. Ha, T.-F. Chan, D. Cai, L. Leung, E. Wan, A. L. Kistler, J. L. DeRisi, P. R. Selvin, and P.-Y. Kwok. Rapid DNA mapping by fluorescent single molecule detection. *Nucleic Acids Res.*, 35(3):e16–e16, 2007.

[23] Ernest T Lam, Alex Hastie, Chin Lin, Dean Ehrlich, Somes K Das, Michael D Austin, Paru Deshpande, Han Cao, Niranjan Nagarajan, Ming Xiao, and Pui-Yan Kwok. Genome mapping on nanochannel arrays for structural variation analysis and sequence assembly. *Nat. Biotechnol.*, 30(8):771–776, 2012.

[24] Gil Henkin, Daniel Berard, Francis Stabile, Marjan Shayegan, Jason S. Leith, and Sabrina R. Leslie. Manipulating and visualizing molecular interactions in customized nanoscale spaces. *Analytical Chemistry*, 88(22):11100–11107, 2016.

[25] Sabrina R. Leslie, Alexander P. Fields, and Adam E. Cohen. Convex lens-induced confinement for imaging single molecules. *Anal. Chem.*, 82(14):6224–6229, 2010. PMID: 20557026.

[26] Daniel J Berard, François Michaud, Sara Mahshid, Mohammed Jalal Ahamed, Christopher M J McFaul, Jason S Leith, Pierre Bérubé, Rob Sladek, Walter Reisner, and Sabrina R Leslie. Convex lens-induced nanoscale templating. *Proc. Natl. Acad. Sci. USA*, 111(37):13295–300, 2014.

[27] Adriel Arsenault, Jason S. Leith, Gil Henkin, Christopher M. J. McFaul, Matthew Tarling, Richard Talbot, Daniel Berard, Francois Michaud, Shane Scott, and Sabrina R. Leslie. Open-frame system for single-molecule microscopy. *Review of Scientific Instruments*, 86(3), 2015.

[28] Daniel J. Berard, Marjan Shayegan, Francois Michaud, Gil Henkin, Shane Scott, and Sabrina Leslie. Formatting and ligating biopolymers using adjustable nanoconfinement. *Appl. Phys. Lett.*, 109(3):033702, 2016.

[29] Tânia E. Sintra, Sónia P.M. Ventura, and João A.P. Coutinho. Superactivity induced by micellar systems as the key for boosting the yield of enzymatic reactions. *J. Mol. Catal. B: Enzym.*, 107:140–151, 2014.

[30] Ashok A Deniz, Samrat Mukhopadhyay, and Edward A Lemke. Single-molecule biophysics: at the interface of biology, physics and chemistry. *J. R. Soc. Interface*, 5(18):15–45, 2008.

[31] Walter Reisner, Jonas N Pedersen, and Robert H Austin. Dna confinement in nanochannels: physics and biological applications. *Rep. Prog. Phys.*, 75(10):106601, 2012.

[32] John F. Thompson and Patrice M. Milos. The properties and applications of single-molecule dna sequencing. *Genome Biol.*, 12(2):1–10, 2011.

[33] Michael L. Metzker. Sequencing technologies — the next generation. *Nat. Rev. Genet.*, 11(1):31–46, 2009.

[34] Andreas Küchler, Makoto Yoshimoto, Sandra Luginbühl, Fabio Mavelli, and Peter Walde. Enzymatic reactions in confined environments. *Nat. Nanotechnol.*, 11(5):409–420, 2016.

[35] Stephen L. Levy and Harold G. Craighead. Dna manipulation, sorting, and mapping in nanofluidic systems. *Chem. Soc. Rev.*, 39:1133–1152, 2010.

[36] Fredrik Persson and Jonas O. Tegenfeldt. Dna in nanochannels-directly visualizing genomic information. *Chem. Soc. Rev.*, 39:985–999, 2010.

[37] Chirlmin Joo, Hamza Balci, Yuji Ishitsuka, Chittanon Buranachai, and Taekjip Ha. Advances in single-molecule fluorescence methods for molecular biology. *Annu. Rev. Biochem.*, 77:51–76, 2008.

[38] Robert K. Neely, Jochem Deen, and Johan Hofkens. Optical mapping of dna: Single-molecule-based methods for mapping genomes. *Biopolymers*, 95(5):298–311, 2011.

[39] Ernest T Lam, Alex Hastie, Chin Lin, Dean Ehrlich, Somes K Das, Michael D Austin, Paru Deshpande, Han Cao, Niranjan Nagarajan, Ming Xiao, and Pui-Yan Kwok. Genome mapping on nanochannel arrays for structural variation analysis and sequence assembly. *Nat. Biotechnol.*, 30(8):771–776, 2012.

[40] Ming Xiao, Angie Phong, Connie Ha, Ting-Fung Chan, Dongmei Cai, Lucinda Leung, Eunice Wan, Amy L. Kistler, Joseph L. DeRisi, Paul R. Selvin, and Pui-Yan Kwok. Rapid dna mapping by fluorescent single molecule detection. *Nucleic Acids Res.*, 35(3):e16, 2007.

[41] Hagar Zohar and Susan J. Muller. Labeling dna for single-molecule experiments: Methods of labeling internal specific sequences on double-stranded dna. *Nanoscale*, 3(8):3027–3039, 2011.

[42] W Cai, H Aburatani, V P Stanton, D E Housman, Y K Wang, and D C Schwartz. Ordered restriction endonuclease maps of yeast artificial chromosomes created by optical mapping on surfaces. *Proc. Natl. Acad. Sci. U.S.A.*, 92(11):5164–5168, 1995.

[43] Jonas O. Tegenfeldt, Christelle Prinz, Han Cao, Steven Chou, Walter W. Reisner, Robert Riehn, Yan Mei Wang, Edward C. Cox, James C. Sturm, Pascal Silberzan, and Robert H. Austin. The dynamics of genomic-length dna molecules in 100-nm channels. *Proc. Natl. Acad. Sci. USA*, 101(30):10979–10983, 2004.

[44] C. Freitag, C. Noble, J. Fritzsche, F. Persson, M. Reiter-Schad, A. N. Nilsson, A. Granéli, T. Ambjörnsson, K. U. Mir, and J. O. Tegenfeldt. Visualizing the entire dna from a chromosome in a single frame. *Biomicrofluidics*, 9(4), 2015.

[45] Kevin D. Dorfman, Scott B. King, Daniel W. Olson, Joel D. P. Thomas, and Douglas R. Tree. Beyond gel electrophoresis: Microfluidic separations, fluorescence burst analysis, and dna stretching. *Chem. Rev.*, 113(4):2584–2667, 2013. PMID: 23140825.

[46] Fabio Baldessari and Juan G. Santiago. Electrophoresis in nanochannels: brief review and speculation. *J Nanobiotechnology*, 4(1):1–6, 2006.

[47] Ahmed Alrifaiy, Olof A. Lindahl, and Kerstin Ramser. Polymer-based microfluidic devices for pharmacy, biology and tissue engineering. *Polymers*, 4(3):1349–1398, 2012.

[48] Ce Zhang, Kai Jiang, Fan Liu, Patrick S. Doyle, Jeroen A. van Kan, and Johan R. C. van der Maarel. A nanofluidic device for single molecule studies with in situ control of environmental solution conditions. *Lab Chip*, 13:2821–2826, 2013.

[49] Ce Zhang, Pei Ge Shao, Jeroen A. van Kan, and Johan R. C. van der Maarel. Macromolecular crowding induced elongation and compaction of single dna molecules confined in a nanochannel. *Proc. Natl. Acad. Sci. U.S.A.*, 106(39):16651–16656, 2009.

[50] Ce Zhang, Durgarao Guttula, Fan Liu, Piravi P. Malar, Siow Yee Ng, Liang Dai, Patrick S. Doyle, Jeroen A. van Kan, and Johan R. C. van der Maarel. Effect of h-ns on the elongation and compaction of single dna molecules in a nanospace. *Soft Matter*, 9:9593–9601, 2013.

[51] Daniel Berard, Christopher M. J. McFaul, Jason S. Leith, Adriel K. J. Arsenault, François Michaud, and Sabrina R. Leslie. Precision platform for convex lens-induced confinement microscopy. *Rev. Sci. Instrum.*, 84:103704, 2013.

[52] Theo Odijk. The statistics and dynamics of confined or entangled stiff polymers. *Macromolecules*, 16(8):1340–1344, 1983.

[53] Douglas R. Tree, Yanwei Wang, and Kevin D. Dorfman. Extension of dna in a nanochannel as a rod-to-coil transition. *Phys. Rev. Lett.*, 110:208103, 2013.

[54] J.K. Armstrong, R.B. Wenby, H.J. Meiselman, and T.C. Fisher. The hydrodynamic radii of macromolecules and their effect on red blood cell aggregation. *Biophys. J.*, 87(6):4259–4270, 2004.

[55] H. Lee, D. Ham, and R.M. Westervelt. *CMOS Biotechnology*. Springer: USA, 2007.

[56] Binu Kundukad, Jie Yan, and Patrick S Doyle. Effect of yoyo-1 on the mechanical properties of dna. *Soft Matter*, 10(48):9721–9728, 2014.

[57] Andy Sischka, Katja Toensing, Rainer Eckel, Sven David Wilking, Norbert Sewald, Robert Ros, and Dario Anselmetti. Molecular mechanisms and kinetics between dna and dna binding ligands. *Biophys. J.*, 88(1):404–411, 2005.

[58] Marcel Reuter and David TF Dryden. The kinetics of yoyo-1 intercalation into single molecules of double-stranded dna. *Biochem. Biophys. Res. Commun.*, 403(2):225–229, 2010.

[59] Katrin Günther, Michael Mertig, and Ralf Seidel. Mechanical and structural properties of yoyo-1 complexed dna. *Nucleic Acids Res.*, 38(19):6526–6532, 2010.

[60] Hays S. Rye, Stephen Yue, David E. Wemmer, Mark A. Quesada, Richard P. Haugland, Richard A. Mathies, and Alexander N. Glazer. Stable fluorescent complexes of double-stranded dna with bis-intercalating asymmetric cyanine dyes: properties and applications. *Nucleic Acids Res.*, 20(11):2803–2812, 1992.

[61] H.S. Rye, J.M. Dabora, M.A. Quesada, R.A. Mathies, and A.N. Glazer. Fluorometric assay using dimeric dyes for double- and single-stranded DNA and RNA with picogram sensitivity. *Anal. Biochem.*, 208(1):144–150, 1993.

[62] M. Maaloum, P. Muller, and S. Harlepp. Dna-intercalator interactions: structural and physical analysis using atomic force microscopy in solution. *Soft Matter*, 9:11233–11240, 2013.

[63] D. Hern Paik and Thomas T. Perkins. Dynamics and multiple stable binding modes of dna intercalators revealed by single-molecule force spectroscopy. *Angew. Chem. Int. Ed.*, 51(8):1811–1815, 2012.

[64] Steven Chu, Stephen R. Quake, and Hazen Babcock. *Nature*, 388(6638):151–154, 1997.

[65] Walter Reisner, Jason P. Beech, Niels B. Larsen, Henrik Flyvbjerg, Anders Kristensen, and Jonas O. Tegenfeldt. Nanoconfinement-enhanced conformational response of

single dna molecules to changes in ionic environment. *Phys. Rev. Lett.*, 99:058302, 2007.

[66] Chih-Chen Hsieh, Anthony Balducci, and Patrick S. Doyle. Ionic effects on the equilibrium dynamics of dna confined in nanoslits. *Nano Lett.*, 8(6):1683–1688, 2008. PMID: 18459741.

[67] Ce Zhang, Fang Zhang, Jeroen A. van Kan, and Johan R. C. van der Maarel. Effects of electrostatic screening on the conformation of single dna molecules confined in a nanochannel. *J. Chem. Phys*, 128(22), 2008.

[68] Andreas S. Biebricher, Iddo Heller, Roel F. H. Roijmans, Tjalle P. Hoekstra, Erwin J. G. Peterman, and Gijs J. L. Wuite. The impact of DNA intercalators on DNA and DNA-processing enzymes elucidated through force-dependent binding kinetics. *Nat. Commun.*, 6:7304, 2015.

[69] S. I. Raider, L. V. Gregor, and R. Flitsch. Transfer of mobile ions from aqueous solutions to the silicon dioxide surface. *J. Electrochem. Soc*, 120(3):425–431, 1973.

[70] Franklin I. Uba, Swathi R. Pullagurla, Nichanun Sirasunthorn, Jiahao Wu, Sunggook Park, Rattikan Chantiwas, Yoon-Kyoung Cho, Heungjoo Shin, and Steven A. Soper. Surface charge, electroosmotic flow and DNA extension in chemically modified thermoplastic nanoslits and nanochannels. *Analyst*, 140(1):113–126, 2015.

[71] Victor A Bloomfield. DNA condensation. *Curr. Opin. Struct. Biol.*, 6(3):334–341, 1996.

[72] Nicholas V. Hud and Igor D. Vilfan. Toroidal dna condensates: Unraveling the fine structure and the role of nucleation in determining size. *Annu. Rev. Biophys. Biomol. Struct.*, 34(1):295–318, 2005. PMID: 15869392.

[73] Sergey M Mel'nikov, Vladimir G Sergeyev, and Kenichi Yoshikawa. Discrete coil-globule transition of large dna induced by cationic surfactant. *J. Am. Chem. Soc.*, 117(9):2401–2408, 1995.

[74] Manfred E. Bayer and Anatoly F. Bocharov. The capsid structure of bacteriophage lambda. *Virology*, 54(2):465–475, 1973.

[75] Alfred Pingoud and Albert Jeltsch. Structure and function of type ii restriction endonucleases. *Nucleic Acids Res.*, 29(18):3705–3727, 2001.

[76] D. Schwartz, X Li, L. Hernandez, S. Ramnarain, E. Huff, and Y. Wang. Ordered restriction maps of saccharomyces cerevisiae chromosomes constructed by optical mapping. *Science*, 262(5130):110–114, 1993.

[77] Robert Riehn, Manchun Lu, Yan-Mei Wang, Shuang Fang Lim, Edward C. Cox, and Robert H. Austin. Restriction mapping in nanofluidic devices. *Proc. Natl. Acad. Sci. U.S.A.*, 102(29):10012–10016, 2005.

[78] Sara Goodwin, John D. McPherson, and W. Richard McCombie. Coming of age: ten years of next-generation sequencing technologies. *Nat. Rev. Genet.*, 17(6):333–351, 2016.

[79] Sara Goodwin, John D. McPherson, and W. Richard McCombie. Coming of age: ten years of next-generation sequencing technologies. *Nat Rev Genet*, 17(6):333–351, 2016.

[80] David C. Bell, W. Kelley Thomas, Katelyn M. Murtagh, Cheryl A. Dionne, Adam C. Graham, Jobriah E. Anderson, and William R. Glover. Dna base identification by electron microscopy. *Microscopy and Microanalysis*, 18:1049–1053, 2012.

[81] Leon M. Bellan, Joshua D. Cross, Elizabeth A. Strychalski, Jose Moran-Mirabal, , and H. G. Craighead. Individually resolved dna molecules stretched and embedded in electrospun polymer nanofibers. *Nano Lett.*, 6(11):2526–2530, 2006. PMID: 17090085.

[82] Aline Cerf, Thomas Alava, Robert A. Barton, and Harold G. Craighead. Transfer-printing of single dna molecule arrays on graphene for high-resolution electron imaging and analysis. *Nano Lett.*, 11(10):4232–4238, 2011. PMID: 21919532.

[83] Stephen R. Wasserman, Yu Tai Tao, and George M. Whitesides. Structure and reactivity of alkylsiloxane monolayers formed by reaction of alkyltrichlorosilanes on silicon substrates. *Langmuir*, 5(4):1074–1087, 1989.

[84] Y.L. Lyubchenko, P.I. Oden, D. Lampner, S.M. Lindsay, and K.A. Dunker. Atomic force microscopy of dna and bacteriophage in air, water and propanol: the role of adhesion forces. *Nucleic Acids Research*, 21(5):1117–1123, 1993.

[85] Yuri L. Lyubchenko, Luda S. Shlyakhtenko, and Toshio Ando. Imaging of nucleic acids with atomic force microscopy. *Methods*, 54(2):274–283, 2011.

[86] Frank Uhlmann. SMC complexes: from DNA to chromosomes. *Nature Reviews Molecular Cell Biology*, 17(7):399–412, 2016.